

RESEARCH

Open Access



# Experimental Seismic Structural Performance Evaluations of RC Columns Strengthened by Stiff-Type Polyurea

Tae-Hee Lee<sup>1</sup>, Seung-Jai Choi<sup>1</sup>, Dal-Hun Yang<sup>2</sup> and Jang-Ho Jay Kim<sup>1\*</sup>

## Abstract

Recently, strong earthquakes are continuously occurring all over the world regarding, repair and strengthening of non-seismically designed structures. Presently, fiber-reinforced polymer (FRP) surface-bonding method is used as a quick and easy way to retrofit and strengthen damaged columns and walls. However, the inherent problems of the FRP surface-bonding method of bond degradation are adhesive interfaces and FRP sheet aging during service-life still. In order to overcome these problems, it is necessary to develop new materials and techniques that can induce monolithic behavior between the structural member and retrofit material by eliminating the bonding interface. One solution is to use repair and strengthening using stiff-type polyurea (STPU) developed as a seismic retrofitting material which can be applied by spraying method. In order to investigate the retrofitting effect of STPU, pseudo-dynamic push-pull test and dynamic shaking table tests are performed. The novelty of the study is that the RC columns strengthened with a newly developed STPU are tested for pseudo-dynamic (i.e., also represents the static behavior) and dynamic behavior. From the test results, overall strengthening effect of the STPU for both static and dynamic loading conditions can be understood, which can be used for retrofitting of concrete structures all over the world. The study results are discussed in detail in the paper.

**Keywords:** seismic, repair, strengthening, retrofitting, polyurea, pseudo-dynamic test, shaking table test

## 1 Introduction

Recently, strong earthquakes with magnitude of over 7.0 on the Richter scale have been reported all over the world (i.e., Haiti earthquake with 7.0 magnitude, Turkey earthquake with 7.3 magnitude, Taiwan earthquake with 7.3–7.6 magnitude, Chile earthquake with 7.8 magnitude, Nepal earthquake with 7.8 magnitude, etc.). These recent earthquakes caused devastating human casualties, critical infrastructures damages, and enormous economic losses (KMA, 2016). In Korea, a recent earthquake of 5.0 magnitude occurred at the eastern sea shore and 5.1

magnitude in the south eastern province (KMA, 2016). Although seismic requirements have been enforced by Korea Road Bridge Design Standard from 1992, only 37% of facilities meet the seismic requirements presently and rest do not satisfy the earthquake requirements, which are in danger of possible damages from earthquake. After the occurrence of Fukushima nuclear disaster induced earthquake in Japan, much attention has been paid to seismic retrofitting of infrastructures and structures in Korea as the demand for seismic retrofitting and strengthening increased (Chung et al., 2002; Jin, 2016; Kim et al., 1997; Lee et al., 2012).

Among representative seismic retrofitting and strengthening methods, such as cross-section enlargement method, reinforcement addition and replacement method, specific member reconstruction method, external surface wrapping method, etc., most extensively used

Journal information: ISSN 1976-0485 / eISSN2234-1315.

\*Correspondence: jjhkim@yonsei.ac.kr

<sup>1</sup> School of Civil and Environmental Engineering, Yonsei University, 50, Yonsei-ro, Seodaemun-gu, Seoul 03722, Republic of Korea  
Full list of author information is available at the end of the article



© The Author(s) 2022. **Open Access** This article is licensed under a Creative Commons Attribution 4.0 International License, which permits use, sharing, adaptation, distribution and reproduction in any medium or format, as long as you give appropriate credit to the original author(s) and the source, provide a link to the Creative Commons licence, and indicate if changes were made. The images or other third party material in this article are included in the article's Creative Commons licence, unless indicated otherwise in a credit line to the material. If material is not included in the article's Creative Commons licence and your intended use is not permitted by statutory regulation or exceeds the permitted use, you will need to obtain permission directly from the copyright holder. To view a copy of this licence, visit <http://creativecommons.org/licenses/by/4.0/>.

method is external surface wrapping method using steel plate and fiber-reinforced polymer (FRP) sheet.

Currently, FRP wrapping method is considered to be the most cost-effective and simple way to improve the load-carrying capacity, ductility, and shear strength of deteriorated concrete members (Almusallam et al., 2018; Bonacci & Maalej, 2001; Chen et al., 2008; Chung et al., 2018; Kim et al., 2013; Lu et al., 2005; Truong et al., 2017; Youm et al., 2006). The FRP surface wrapping method gives confinement effect and stiffness enhancement to resist seismic loading. The external wrapping material can be categorized into stiff and ductile type of steel plate and FRP sheet, respectively. Researches on the surface wrapping using ductile type material (DTM) started in Japan. FRP sheet wrapping is effective due to its high tensile strength property, which applies continuous confinement pressure to the deteriorated member while maintaining its elastic behavior. One example of the effectiveness of FRP surface wrapping method was verified through Sanriku Shore Japan earthquake with 7.5 magnitude on March 11, 2011. The reinforced concrete columns retrofitted by surface wrapping of FRP sheet survived the earthquake without extensive damage, while the columns surface wrapped by steel plate had extensive concrete spalling and member damage. Although the retrofitting and strengthening by surface wrapping FRP sheet on deteriorated concrete member are effective, the long-term effectiveness of the method has been questioned due to service life of bonding epoxy and resin impregnated between fibers from weathering. More specifically, the concrete members exposed to continuous outside environmental conditions of sunlight, wind, storm, temperature and humidity variations, etc., cause the deterioration of the bonding epoxy and surface wrapped FRP sheet to the point of retrofitting becoming meaningless. In order to overcome these problems, a new surface coating material without bonding interface and binding requirement is needed. One material that can solve this problem is polyurea (PU), which has equivalent material characteristics as FRP sheet, but do not require interface bonding and binding requirement. PU has good tensile strength with ductile property to give continuous confinement effect to the deteriorated concrete member. Also, various study reports stated that the long-term characteristics of PU under outside weather conditions are excellent and can be used for 10–15 years (Huang et al., 2012; Zhang et al., 2006).

Therefore, in this study stiff-type PU (STPU) developed for seismic retrofitting is applied to reinforced concrete (RC) specimens to be evaluated under seismic loading. STPU is a newly developed seismic retrofitting material by modifying the physical properties of PU (e.g.,

a polymer material with high-ductile and high-tensile strength properties) using highly polymerized compounds. Also, since STPU alone cannot apply sufficient strength and stiffness to large size RC members needed in civil infrastructures such as bridge girders and columns, a hybrid method of using both STPU and glass fiber-reinforced polymer (GFRP) sheet (e.g., STPU on top of GFRP sheet) is proposed. Especially, STPU sprayed on top of wrapped GFRP sheet will protect GFRP from deteriorating under weathering conditions.

To evaluate the strengthening effectiveness of STPU only and hybrid GFRP-STPU (GFPU), quasi-static, pseudo-dynamic, and shaking table tests are conducted on the RC column model specimens. The basic concepts of the pseudo-dynamic test were proposed by Hakuno, and the computer-based technique was proposed for the study of the inelastic dynamic behavior of the structure against seismic load. Many studies on seismic performance have been conducted in recent years using the pseudo-dynamic test by improving on the method's shortcomings (Ang et al., 1989; Chen et al., 2003; Jung et al., 2006; Li et al., 2003; Marriott et al., 2009; Shing & Vannan, 1991; Yang et al., 2004). Quasi-static and pseudo-dynamic tests were performed on GFPU-strengthened 1/2 scale model RC column specimens by applying cyclic loading. Also, shaking table test was performed on a 1/6-scale GFPU-strengthened RC column specimens by applying El Centro seismic acceleration data. Based on the test results, the seismic strengthening performance of STPU surface wrapping is determined by comparing with the test results of non-strengthened RC column specimens. The experiments carried out in the study are to understand the strengthening effect of polyurea applied to rectangular and circular RC columns for both quasi-dynamic and dynamic loading conditions.

## 2 Strengthening Evaluation Test Specimen Details

The target bridge was an 8-span continuous slab bridge in which each column was  $\Pi$  shape with circular cross-section; the P4 column was selected as the target test column. For this column, H/D was 5.83, considerably longer than the 3.0 specified in the classification criteria of slender columns. Using a conformity ratio of 1:2, a scaled model of circular and rectangular cross-sectional column was designed. The same compression load was designed to be applied to scaled models of both circular and rectangular cross-sectional columns. Table 1 presents a conformity ratio by physical quantity applied to the design, and Table 2 summarizes the dimension of the specimens of circular and rectangular half-scale models. The scaling of 1/2 and 1/6 models are selected to reduce the specimen size as much as possible while the column

**Table 1** Similarity of pseudo-dynamic test.

Quality	Dimension	Scale factor
Length	M	S
Mass	M	S <sup>3</sup>
Force	MLT <sup>-2</sup>	S <sup>2</sup>
Stress	ML <sup>-1</sup> T <sup>-2</sup>	1
Velocity	LT <sup>-1</sup>	1
Acceleration	LT <sup>-2</sup>	S <sup>-1</sup>
Time	T	S

behaviors under pseudo-dynamic and dynamic loading, respectively, are maintained. Although the dynamic behavior would have been more clearly shown in a larger dynamic specimen such as 1/2 or ¼-scale specimen, the only available shaking table that can be used for the test was a machine that can only bare up to 1/6-scale specimen. In order to compensate for the small dynamic specimen size, a very large weight mass is placed on the top of the column by anchoring to the specimen using a pre-stressing tendon at the center of the cross-section of the full length of the column. The very heavy weight at the top of the column would induce the mass acceleration effect of the specimen, which would show the seismic or dynamic strengthening effect of the polyurea. Concrete with design compressive strength of 30 MPa was used to cast the specimens. Also, an axial load of 38.75 tons was applied to the column specimen by prestressing two steel wire strands in the vertical direction. The same axial compressive load was applied to both circular and rectangular column specimens. The steel strand used for the axial load was SWPC 7-strand B type (1860 MPa) with a diameter of  $\phi 15.2$  mm, yield strength of 1600 MPa, ultimate strength of 1730 MPa, and unit weight of 1.101 kg/m.

## 2.1 Half-Scale Model Column Specimen Details

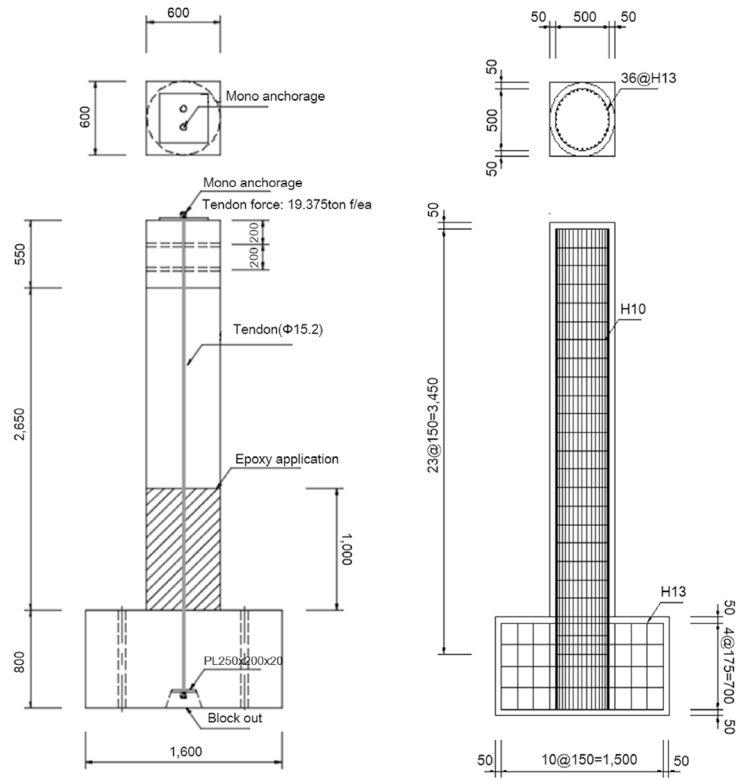
One circular cross-sectional RC column specimen without strengthening in half-scale to the target column was used in the quasi-static test. Total of six half-scale column specimens (3 circular and 3 rectangular column specimens) were used in the pseudo-dynamic test. Figs. 1 and 2 show the plan view and details of circular and rectangular half-scale RC specimen, respectively. For circular cross-sectional columns with a cross-sectional diameter of 600 mm and a height of 2900 mm, 36-D13 longitudinal rebars and D10 hoop ties with 150 mm spacing were placed. Considering the reinforcement ratio of 0.0161 of the target column, the reinforcement ratio was designed and manufactured to be 0.0161. For rectangular cross-sectional columns with a width, a length, and a height of 540 mm, 680 mm, and 2,900 mm, respectively, 46-D13 longitudinal rebars and D10 tie hoop ties with spacing of 150 mm were placed. Considering a reinforcement ratio of 0.0161 of the target column, a reinforcement ratio was designed and manufactured to be 0.0158.

## 2.2 One-Sixth Scale Model Column Specimen Details

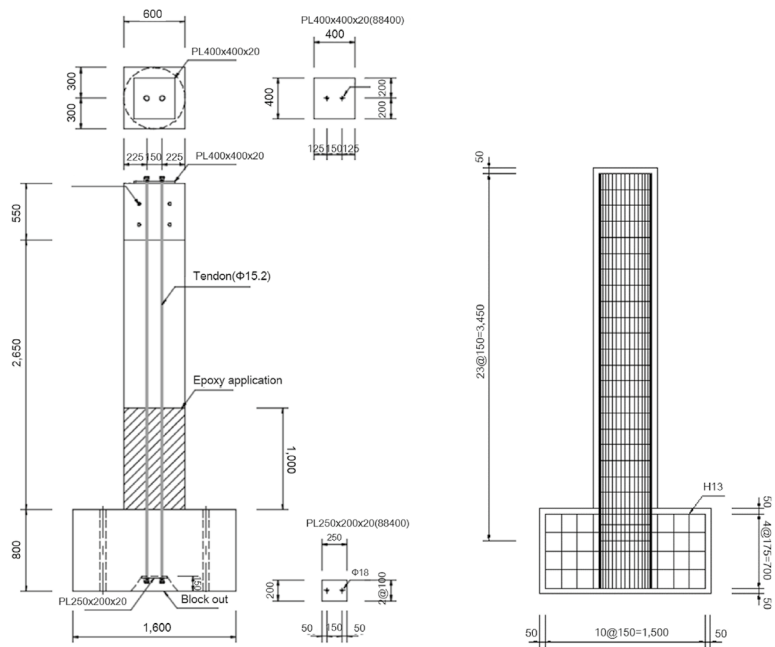
Total of six 1/6-scale column specimens (3 circular and 3 rectangular cross-sectional column specimens) were used in shaking table test. Table 3 summarizes dimensions and details of the circular and rectangular specimens in one-sixth scale. Figs. 3 and 4 show the plans of circular and rectangular column specimens, respectively. For circular cross-sectional columns with a cross-sectional diameter of 200 mm and a height of 1025 mm, eight longitudinal D10 rebars and D10 hoop ties with 75 mm spacing were placed. Considering the reinforcement ratio of 0.0161 of the target column, the reinforcement ratio was designed and manufactured to be 0.0182. For rectangular cross-sectional column specimens with

**Table 2** Specification of circular and rectangular column specimens (similarity, 1:2).

Quality	Target column	Circular cross-sectional column specimen	Similarity	Rectangular cross-sectional column specimen
Section (mm)	Diameter	Diameter		Length × breadth
	1200	600	2	540 × 680
Height (mm)	6100	2900	2.10	2900
Geometry ratio	5.08	5.08	1	5.08
Axial load (ton)	155	38.75	2	38.75
Longitudinal reinforcing bar (mm)	D25 = 25.4	D13 = 12.7	2	D13 = 12.7
Ratio of reinforcement	0.016129	0.016132	0.99, 1.01	0.015872
Hoop reinforcing bar (mm)	D13 = 12.7	D10 = 9.53	1.33	D10 = 9.53
Spacing of hoop (mm)	S = 300	S = 150	2	S = 150

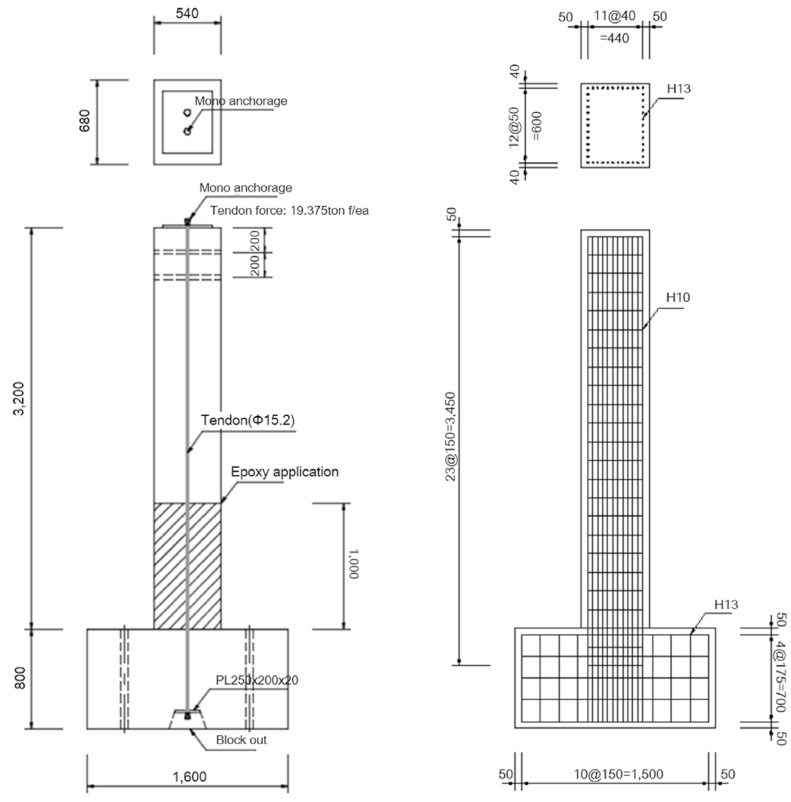


(a) Side view

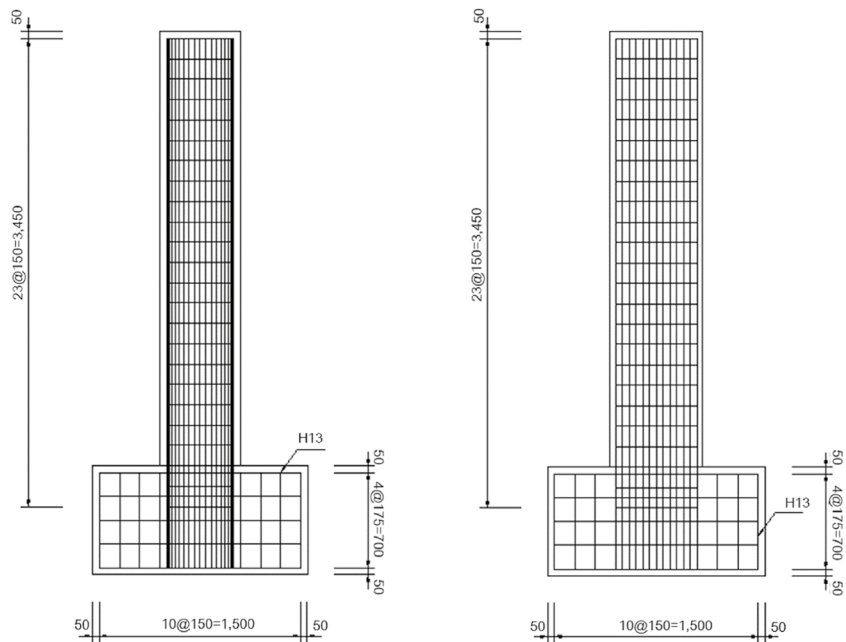


(b) Front view

**Fig. 1** Details of 1/2-scale model circular cross-sectional RC column specimens.



(a) Side view



(b) Front view

**Fig. 2** Details of 1/2-scale model rectangular cross-sectional RC column specimens.

**Table 3** Specification of circular and rectangular column specimens (similarity, 1:6).

Quality	Target column	Circular cross-sectional column specimen	Similarity	Rectangular cross-sectional column specimen
Section (mm)	Diameter 1200	Diameter 600	2	Length × breadth 540 × 680
Height (mm)	6100	1025	5.95	1025
Axial load (ton)	155	4.305	6	4.305
Longitudinal reinforcing bar (mm)	D25 = 25.4	D10 = 9.53	2.66	D10 = 9.53
Ratio of reinforcement	0.016129	0.01817	0.88, 0.90	0.01801
Hoop reinforcing bar (mm)	D13 = 12.7	D10 = 9.53	1.33	D10 = 9.53
Spacing of hoop (mm)	S = 300	S = 75	4	S = 75

width, length, and height were 180 mm, 220 mm, and 1025 mm, respectively, 10-D10 longitudinal rebars and D10 hoop ties with 75 mm spacing were placed. Considering a reinforcement ratio of 0.0161 of the target column, a reinforcement ratio was designed and manufactured to be 0.0180. Fig. 5 shows the photo of a front view of the specimens for shaking table test.

### 2.3 STPU and GFPU-Strengthening Details

Two strengthening methods are proposed: (1) STPU sprayed on concrete surface only (STPU) and (2) wrapping GFRP sheets on concrete surface followed by spraying STPU on top of GFRP sheet (GFPU) as shown in Fig. 6a and b, respectively. For pseudo-dynamic and shaking table test, the strengthening material thickness of 5 mm is applied up to 1000 mm and 400 mm height from the base of the column, respectively. STPU have high tensile strength and low percent elongation. The material properties of STPU, rebar, tendon, and concrete are presented in Table 4. Tables 5 and 6 present an outline of the pseudo-dynamic and shaking table test specimens according to strengthening type, respectively. The nomenclature of the specimens is R- or C- followed by either RC, PU, or GFPU. R- or C- represents rectangular or circular cross-section shape, respectively. RC, PU, or GFPU represents non-strengthened, PU-only strengthened, or GFPU-strengthened specimens, respectively. Fig. 7 shows the photos of the strengthened specimens.

### 2.4 Data Measurement Details

For tendon and steel strain measurement, Tokyo Sokki strain gauges are used. And for the measurement of displacement, 1000-mm wire type LVDT are placed on the top of the column for the quasi-dynamic test while the same LVDTs are placed at the middle and bottom of the column for the dynamic test.

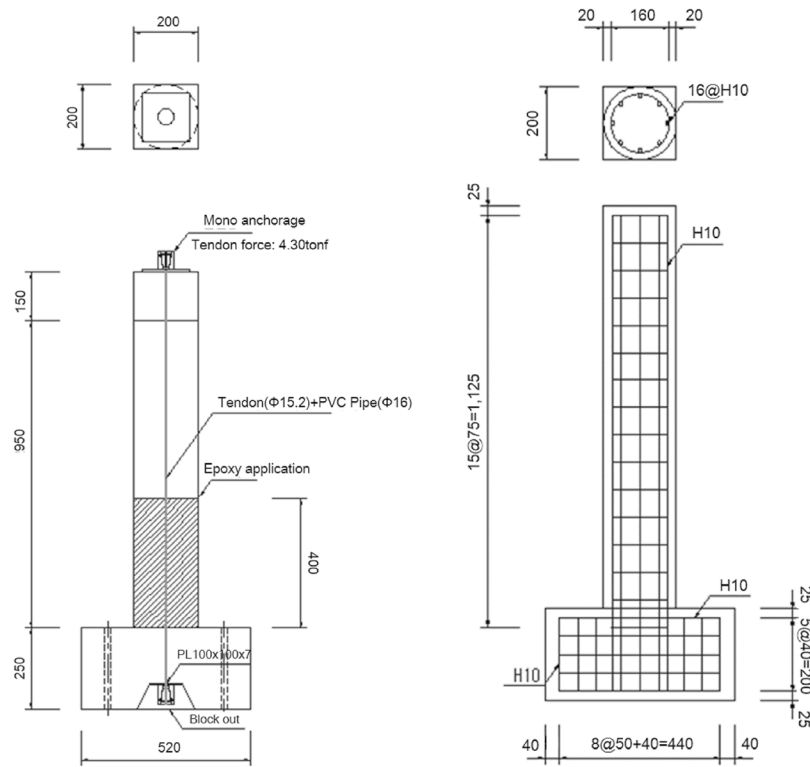
The data logger used in the experiment was TDS-303, a measurement equipment manufactured by Tokyo Sokki, Japan. TDS-303 is an equipment for the purpose of automatic switching measurement of multi-points such as strain gauge, DC voltage, thermocouple, and platinum resistance thermometer. In addition, the concrete gauge used in the experiment is a P-type strain gauge and is used to measure behavior of concrete and mortar specimen or the static modulus of elasticity. Fig. 8 shows the TDS-303 and P-type strain gauges.

#### 2.4.1 Pseudo-dynamic Test Specimen

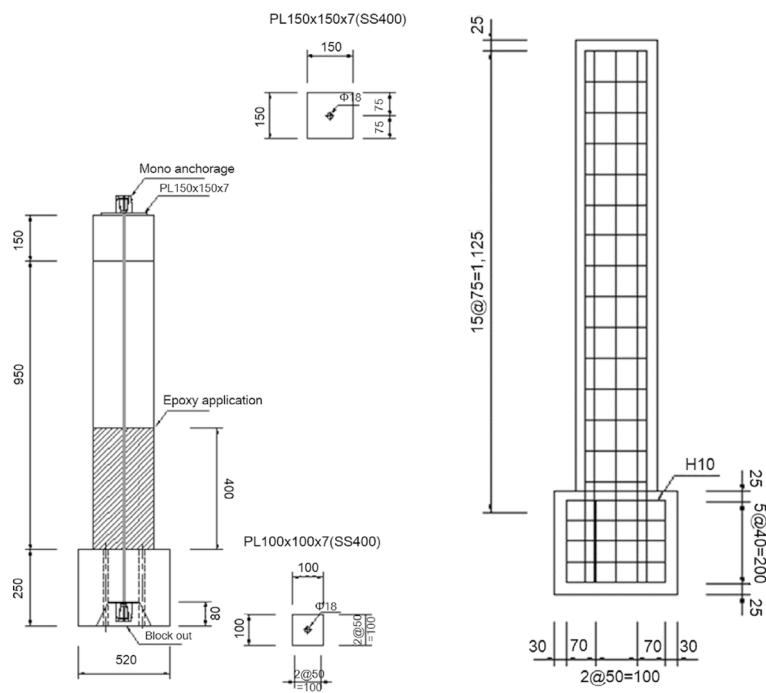
In order to measure deflections and strains of strengthened model column specimens under seismic loading in pseudo-dynamic test, LVDTs and strain gauges were used. As shown in Fig. 9a, a total of six LVDTs were placed. A 1000-mm wire type LVDT was installed at the top of the column specimen to measure a load point displacement history. Similarly, a 200-mm LVDT at the column center, two 100-mm LVDTs at 500 mm and 250 mm from the column base (e.g., STPU-retrofitted height of 1000 mm from the column base), and two 50-mm LVDTs at 1/2 location of footing height. Three strain gauges per specimen were attached on prestressing strand at the top, mid-height, and 500 mm from the column base locations as shown in Fig. 9b. The locations of rebar strain gauge are shown in Fig. 10. Thirty and 22 strain gauges were installed in the circular and square cross-sectional column specimen, respectively, as shown in Fig. 10a and b, respectively.

#### 2.4.2 Shaking Table Test Specimen

In order to measure deflections and strains of strengthened model column specimens under El Centro earthquake loading in shaking table test, LVDTs, strain gauges, accelerometers were used. As shown in Fig. 11a, three

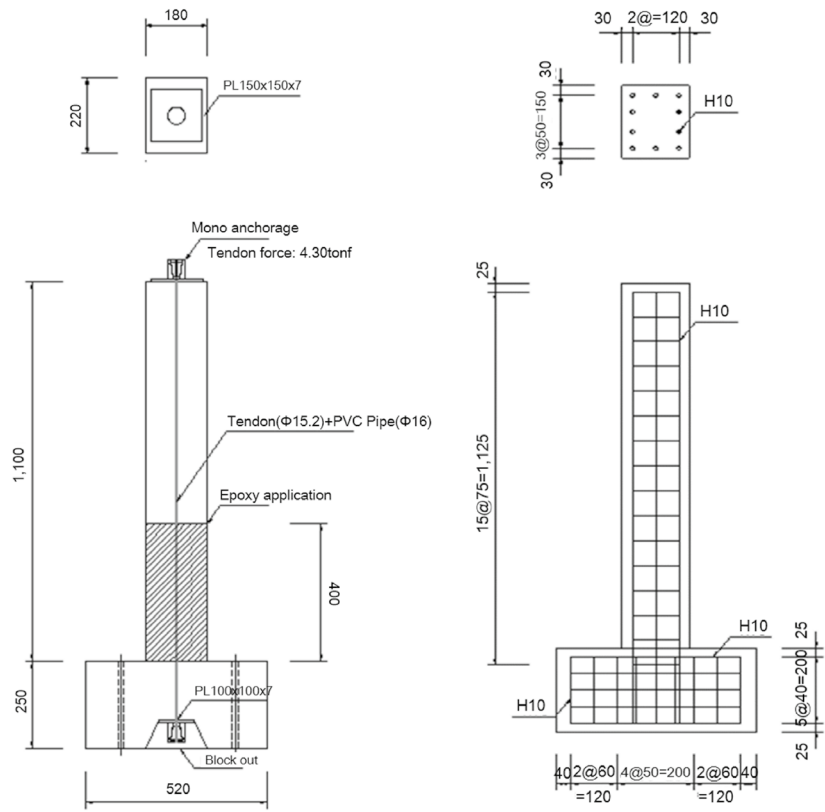


(a) Side view

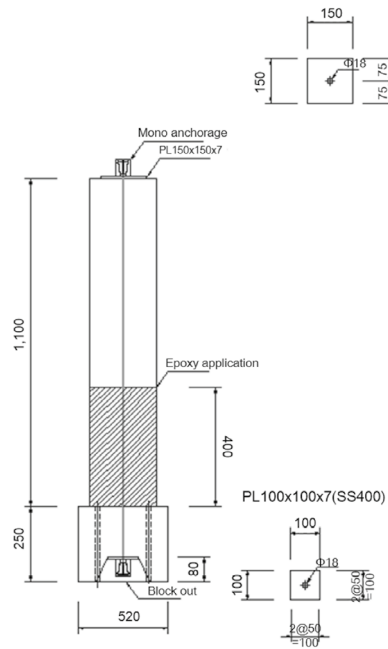


(b) Front view

**Fig. 3** Details of 1/6-scale model circular cross-sectional RC column specimens.



(a) Side view



(b) Front view

**Fig. 4** Details of 1/6-scale model rectangular cross-sectional RC column specimens.



**Fig. 5** Front view of specimens of shaking table test

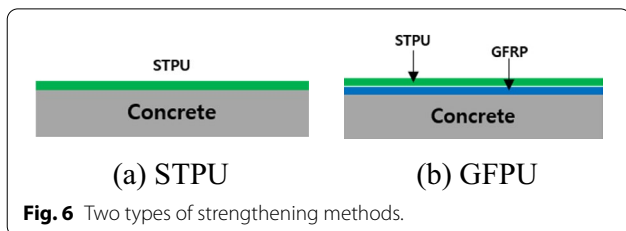


**Fig. 6** Two types of strengthening methods.

**Table 4** Material properties of STPU.

Properties	STPU	Concrete	Rebar	Tendon
Drying time (s)	20	–	–	–
Tensile strength (MPa)	26	2.8	400	1600
Shore hardness (D)	70	–	–	–
Bond strength (MPa)	14	–	–	–
Percent elongation	150	–	–	–
Compressive strength (MPa)	–	30	–	–

**Table 5** Outline of specimens of quasi-static and pseudo-dynamic test.

Specimen	Cross-section type	Strengthened type	Test
C-RC	Circular	RC	Quasi-static
C-RC	Circular	RC	Pseudo-dynamic
R-RC	Rectangular	RC	Pseudo-dynamic
C-PU	Circular	STPU 5 mm	Pseudo-dynamic
R-PU	Rectangular	STPU 5 mm	Pseudo-dynamic
C-GFPU	Circular	GFPU (GFRP + STPU) 5 mm	Pseudo-dynamic
R-GFPU	Rectangular	GFPU (GFRP + STPU) 5 mm	Pseudo-dynamic

RC: non-strengthened, C-: circular column, R-: rectangular column.

LVDTs and two accelerometers were placed. A 1000-mm wire type LVDT was placed at the top of the specimen. A 1000-mm LVDT was placed at 200 mm from the column base (e.g., STPU-retrofitted height of 400 mm from the column base), and a 1000-mm LVDT was placed at the mid-height of the shaking table to measure table displacement history. Two 1.0 g accelerometers were attached at the top and 200 mm from the column base. Two strand gauges per specimen were attached on prestressing strand at mid-height and 200 mm from the column base locations as shown in Fig. 11b. The locations of rebar strain gauge are shown in Fig. 12. A total of 24 strain gauges per specimen were installed as shown in Fig. 12.

### 3 Quasi-static Test

In order to determine the elastic–plastic hysteresis behavior of the specimens, a quasi-static test was conducted. For the horizontal loading, the displacement control load was applied to measure a drift level based on displacement at the top of the specimen. The drift level was increased by 0.25% in every two cycles before proceeding to the next load step. The displacement–time history based on displacement control loading is shown in Fig. 13. A hydraulic loading device (maximum stroke  $\pm 250$  mm, maximum loading 1000 kN) was used in the test with a constant axial load of 38.75 tons applied by 2 prestressed strands in the vertical direction.

#### 3.1 Half-Scale Model Column Specimen Details

A quasi-static test was conducted to model numerical analysis on non-elastic behaviors of a half-scale circular cross-sectional RC column specimen. Fig. 14 shows a load–displacement behavior in the quasi-static test. The maximum displacement of 69.23 mm and 61.46 mm occurred under the maximum push load of 196.04 kN and the maximum pull load of 179.57 kN, respectively. The initial stiffness and mechanical properties were calculated by substituting the test data into the stiffness matrix.

**Table 6** Outline of specimens of shaking table test.

Specimen	Cross-section type	Strengthened type	Test
C-RC	Circular	RC	Shaking table
R-RC	Rectangular	RC	Shaking table
C-PU	Circular	STPU 5 mm	Shaking table
R-PU	Rectangular	STPU 5 mm	Shaking table
C-GFPU	Circular	GFPU (GFRP + STPU) 5 mm	Shaking table
R-GFPU	Rectangular	GFPU (GFRP + STPU) 5 mm	Shaking table

RC: non-strengthened, C-: circular column, R-: rectangular column.

### 4 Pseudo-dynamic Test

For input acceleration in the pseudo-dynamic test, 1940, El Centro earthquake acceleration curve shown in Fig. 15 was used. The peak ground acceleration (PGA) was 0.35 g and total excitation time was 31.2 s.

In the pseudo-dynamic test, 0.7 g acceleration (e.g., two folds of the maximum PGA of El Centro earthquake) was applied. The unit integration time was 0.02 s and damping ratio was 5%. The results obtained from the quasi-static test were used to set initial stiffness and frequency in the input data. Open System for Earthquake Engineering Simulation (OpenSees) was used for the analysis. Newmark- $\beta$  was used as the time-integration method to conduct the test.

### 4.1 Test Results and Discussion

#### 4.1.1 Force Versus Displacement Curve and Relative Displacement

0.7 g acceleration, which was twice that of the PGA of the El Centro EQ (PGA=0.35 g), was applied to all specimens. Fig. 16 shows load–displacement curves in which 0.7 g was applied to circular and rectangular cross-sectional specimens during the pseudo-dynamic test. Table 7 presents displacements for specimens according



(a) RC



(b) PU



(c) GFPU

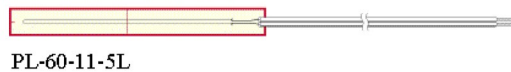


(d) Spraying STPU

**Fig. 7** Types of strengthening material.



(a) Concrete static strain measuring equipment (TDS-303)



(b) P-type Concrete strain gauge (PL-60-11-5L)

**Fig. 8** Data measurement for restrained drying shrinkage test.

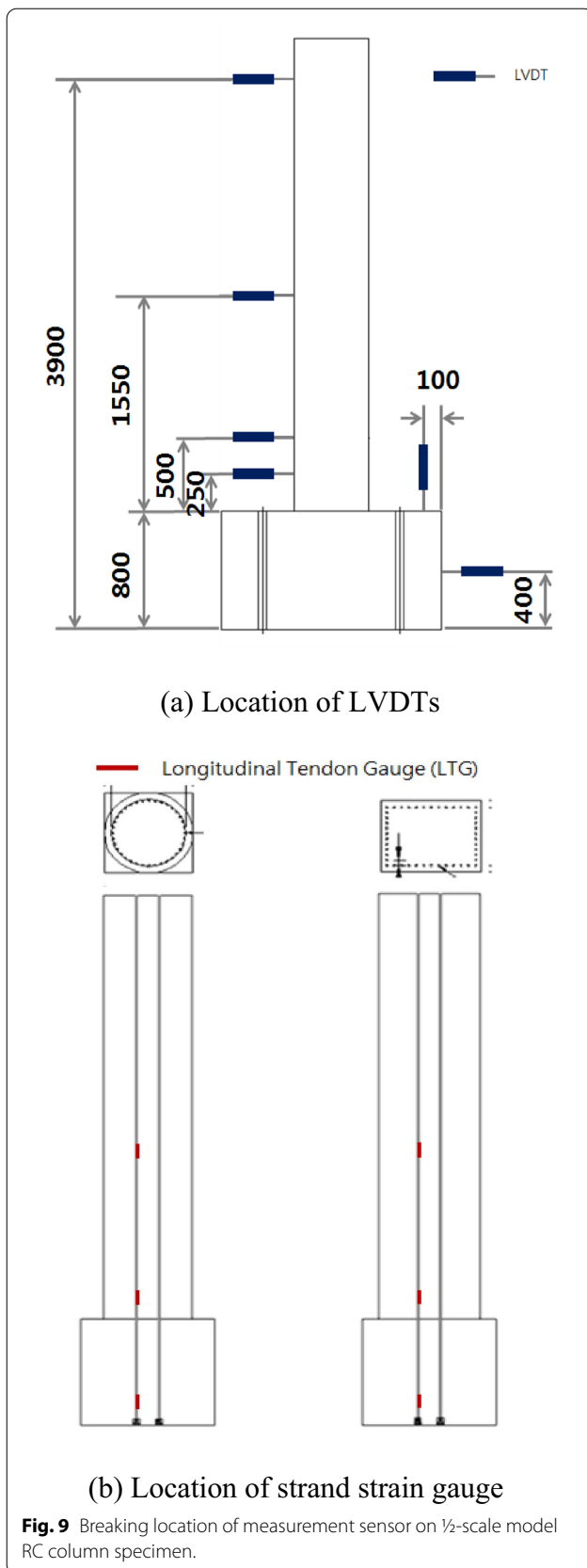
to the maximum load. The results of relative displacement calculation from the maximum load in the push direction to the pull direction for C-RC, C-PU, C-GFPU, R-RC, R-PU, and R-GFPU were 124.00 mm, 118.51 mm, 114.99 mm, 105.89 mm, 100.06 mm, and 96.18 mm, respectively. Compared to non-strengthened RC specimens, the displacements of the circular and rectangular PU-strengthened specimens decreased by 4% and 6%, respectively. Compared to non-strengthened RC specimens, the displacements of the circular and rectangular GFPU-strengthened specimens decreased by 7% and 9%, respectively. As expected, the comparison results showed that the GFPU-strengthening is more effective than PU-only strengthening.

Fig. 17 shows a displacement–time curve of circular and rectangular cross-sectional specimens during the pseudo-dynamic test. Both of the circular and rectangular specimens showed residual slanting failure deformation toward the pull direction after the seismic test. The residual deflections at the load point for C-RC, C-PU, C-GFPU, R-RC, R-PU, R-GFPU specimens were 20.91 mm, 10.31 mm, 6.79 mm, 20.69 mm, 9.58 mm, and 8.25 mm, respectively. The residual deflections in the rectangular PU and GFPU-strengthened specimens decreased by 53.7% and 60.1% compared to

non-strengthened specimen, respectively. The difference between PU and GFPU-strengthened rectangular specimens was 1.33 mm equivalent to 6.4% less for GFPU specimen. The residual deflections in the circular PU and GFPU-strengthened specimens decreased by 50.7% and 60.5% compared to non-strengthened specimen, respectively. The difference between PU and GFPU-strengthened rectangular specimens was 3.52 mm equivalent to 9.8% less for GFPU specimen. As expected, the best strengthening performance was observed in the GFPU-strengthened specimens. Also, the better strengthening performance was observed in the GFPU-strengthened circular column than rectangular column due to the continuous confinement effect in circular column for not having sharp corners in the cross-section. Also, the test results showed that the strengthening specimens had higher stiffness than the non-strengthened specimens under seismic loading.

#### 4.1.2 Rebar Strains

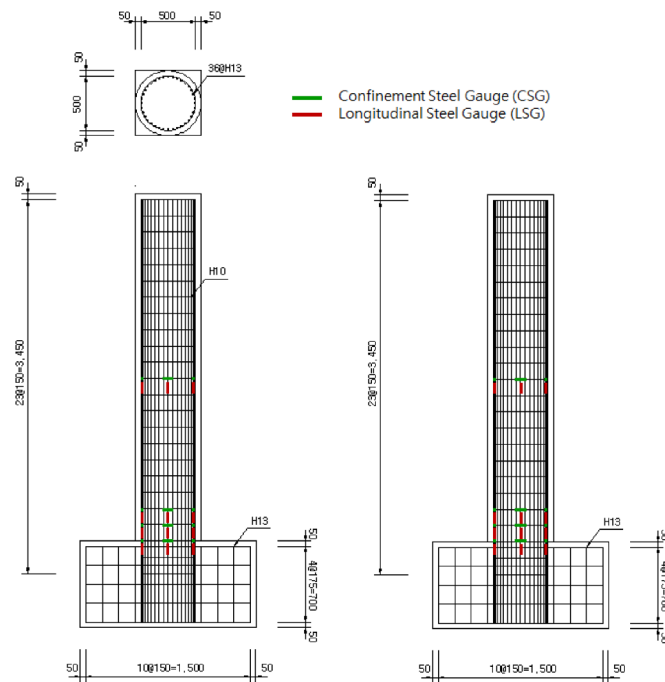
Figs. 18 and 19 show the load–strain curves of the main rebar strains in all specimens during the pseudo-dynamic test. Table 8 presents the strain data of the specimens according to the maximum load. Compared to non-strengthened RC specimens, the strain of



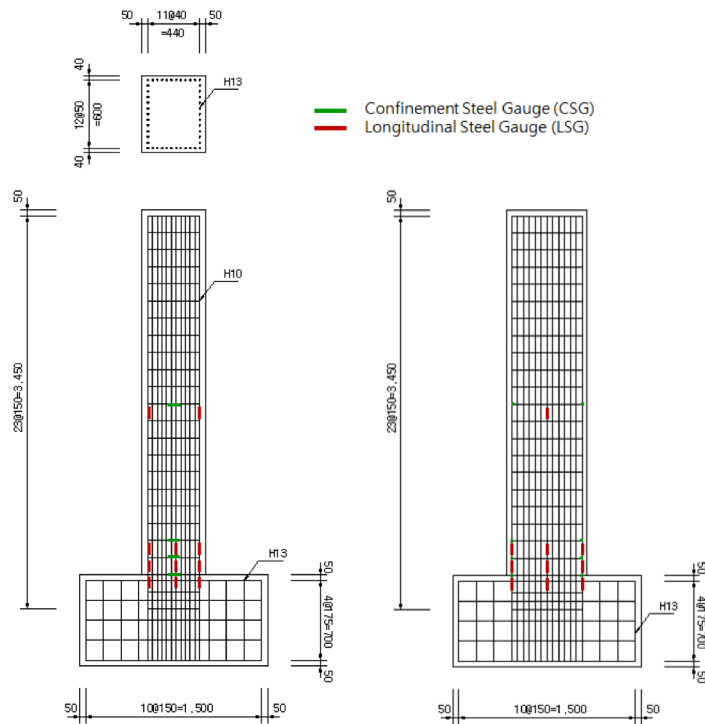
PU-strengthened circular and rectangular specimens decreased by 16–43% and 15–26%, respectively. On the other hand, the strain of GFPU-strengthened circular and rectangular specimens decreased by 0–28% and 5–23%, respectively. The rebar strain results showed that PU- and GFPU-strengthened of circular and rectangular specimens significantly improved under seismic loading.

Tables 9 and 10 show the main rebar strains in terms of stress for the circular and rectangular specimens, respectively. The stress magnitudes of the main rebars under the same applied load magnitude are in the following order of non-strengthened RC, PU-strengthened, and GFPU-strengthened specimens with the non-strengthened RC specimen being the largest. In the push direction (e.g., rebar in tension), the rebar in C-RC specimens yielded at the load of 50 kN with the rebar strain of 152.71 MPa (e.g., the allowable stress threshold of SS400 steel rebar is 140 MPa). The strengthened circular specimen began to yield when the load reached 90 kN with the rebar stresses of 133.7 MPa and 126.18 MPa for C-PU and C-GFPU specimens, respectively. The corresponding rebar stress at the same load for C-RC specimen was 232.52 MPa. In the pull direction (e.g., rebar in compression), the rebars of C-RC and C-PU specimens yielded when the load reached 40 kN with the rebar strain of 170.89 MPa and 160.38 MPa, respectively. However, the main rebar of C-GFPU specimen yielded at the load of 50 kN with the stress of 174.14 MPa. The corresponding rebar stresses at the same load for C-RC and C-PU specimens were 211.12 MPa and 194.77 MPa, respectively. For rectangular specimens in push direction, the rebar in R-RC, R-PU, and R-GFPU yielded at the load of 120 kN, 190 kN, and 180 kN, respectively, with the stress of 142.86 MPa, 142.07 MPa, and 142.62 MPa, respectively. In the pull direction, the rebar in R-RC and R-PU specimens yielded at the load of 70 kN with the stress of 167.03 MPa and 170.99 MPa, respectively. However, the rebar in R-GFPU specimen yielded at the load of 90 kN with the stress of 165.57 MPa. The corresponding rebar stresses at the same load for R-RC and R-PU specimens were 204.44 MPa and 199.97 MPa, respectively.

Both the circular and rectangular specimens showed a significant strengthening effect in resisting tensile strains and stresses. GFPU specimens performed better than PU specimens in resisting compressive strains and stresses. Due to the existence of four corners in the rectangular specimens, the lateral stiffness of the specimens was greater than that of the circular specimens, resulting in less lateral deflections in rectangular specimens than the circular specimens. For this cross-sectional stiffness effect, the absolute rebar strains and stresses were greater in the circular specimen than the rectangular specimens.

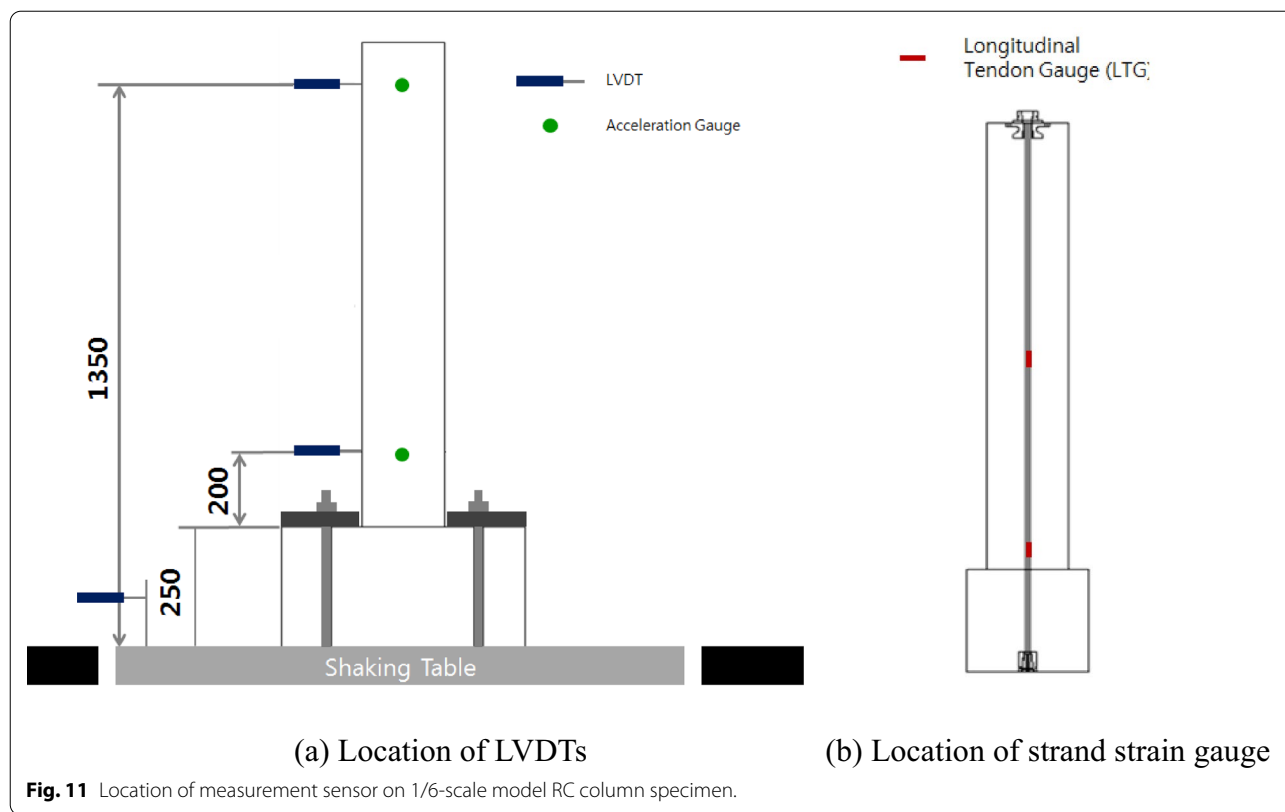


(a) Circular cross-sectional RC column specimen



(b) Rectangular cross-sectional RC column specimen

**Fig. 10** Steel gauge location on 1/2-scale model RC column specimen.



However, the relative strengthening effect was similar for both the circular and rectangular specimens.

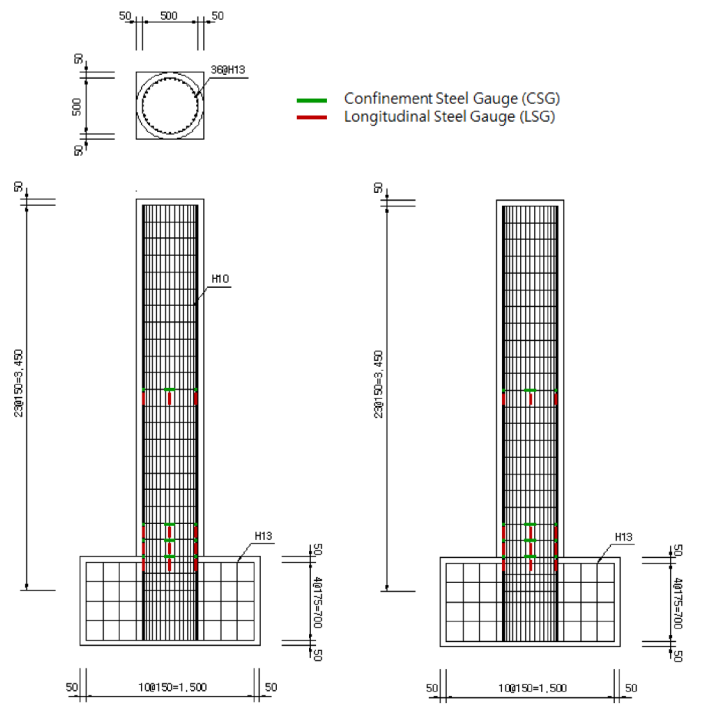
#### 4.1.3 Displacement Ductility

Load–displacement envelope curves up to the maximum load of all specimens are shown in Figs. 20 and 21. Usually, displacement ductility is calculated as a ratio of displacement difference between maximum and yield displacements divided by yield displacement. However, in this study, displacement ductility is calculated as maximum displacement divided by yield displacement (MacRae & Kawashima, 1997). Table 11 presents calculated displacement ductility for all tested specimens. For circular specimens, displacement ductility of PU- and GFPU-strengthened specimens improved by 1.16–1.48 times and 1.22–1.37 times, respectively, compared to non-strengthened RC specimen. For GFPU-strengthened specimens, the ductility was less than the PU specimens, because the stiffness of the GFPU-strengthening material was higher than PU-strengthening material. For rectangular specimens, displacement ductility of PU-strengthened and GFPU-strengthened specimens were 0.93 times

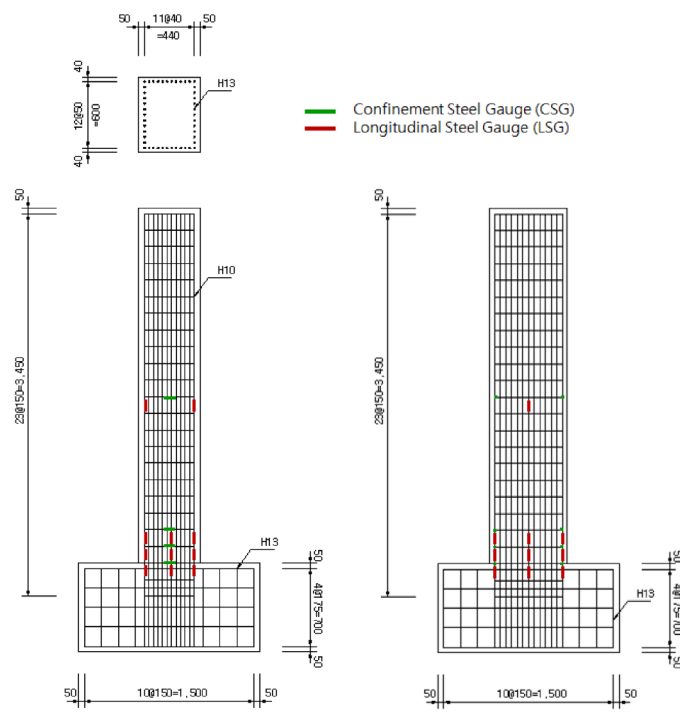
and 0.88 times to that of non-strengthened RC specimen, respectively. Fig. 22 shows failure behavior of specimens of pseudo-dynamic test. The lower ductility comes from the tearing of the strengthening region at the sharp corners in the rectangular section as shown in Fig. 22e and f, respectively, thereby reducing confinement effect and composite behavior between the strengthening material and the RC column specimen. However, in the circular specimens without corners, the ductility of the strengthened specimens was higher than the non-strengthened specimens due to the survival of the strengthening region (e.g., without tearing and premature failure) throughout the test.

#### 4.1.4 Dissipation Energy

Energy absorption and dissipation capacity of the specimen is most important indicator of seismic performance. Dissipation energy is defined as an area under load–displacement history curve. Table 12 summarizes calculated dissipation energy from the load–displacement history curves obtained from the test (Fig. 16). For the circular specimens, the dissipation energy of



(a) Circular cross-sectional RC column specimen



(b) Rectangular cross-sectional RC column specimen

**Fig. 12** Steel gauge location on 1/6-scale model RC column specimens.

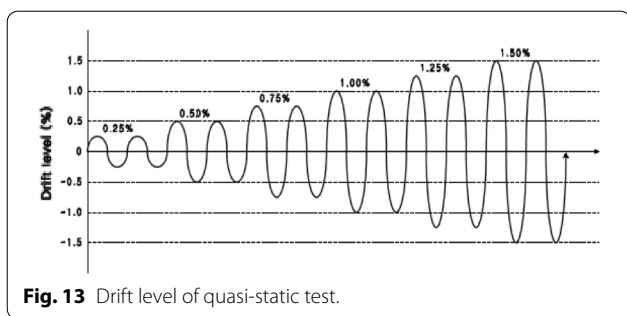


**Fig. 13** Drift level of quasi-static test.

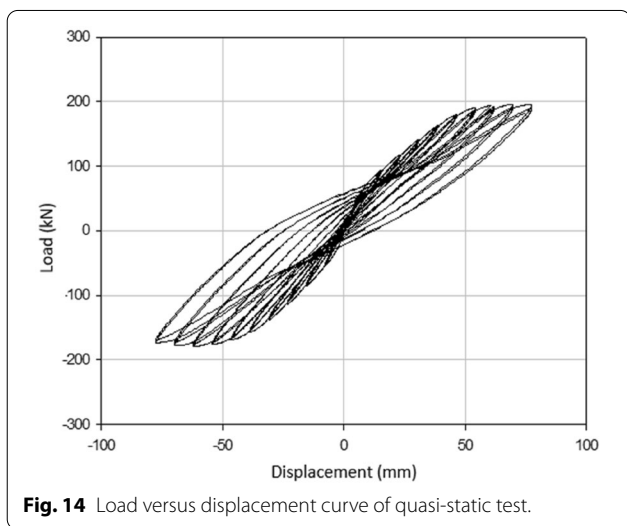


**Fig. 14** Load versus displacement curve of quasi-static test.

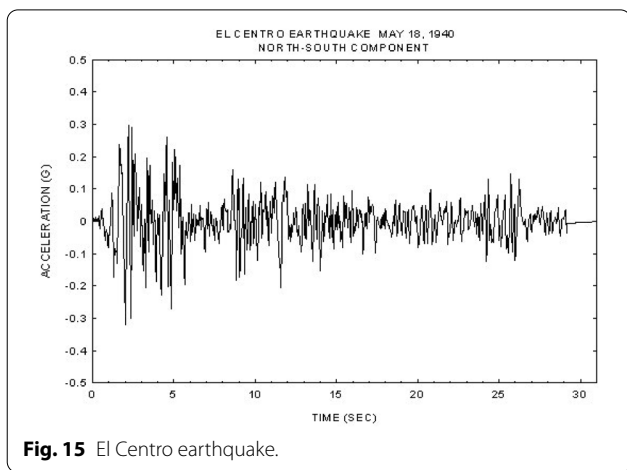


**Fig. 15** El Centro earthquake.

PU-strengthened and GFPU-strengthened specimens were 1.53 and 1.52 compared to that of non-strengthened RC specimen, respectively. For rectangular specimens, the dissipation energy of PU-strengthened and

GFPU-strengthened specimens were 0.83 and 0.74 compared to that of non-strengthened RC specimen, respectively. As explained previously, this inverse behavior was due to premature tearing failure of both PU and GFPU-strengthening region at the sharp corners of the rectangular section.

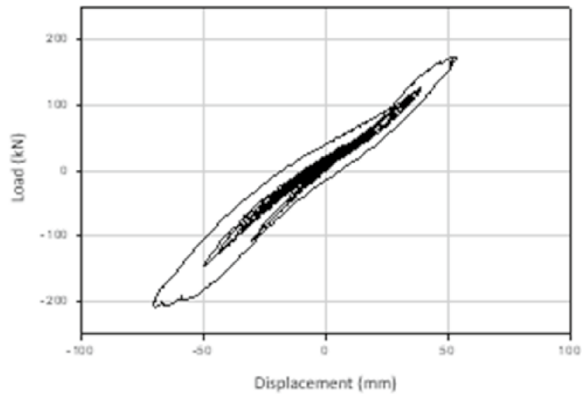
### 5 Shaking Table Test

The experimental equipment for the one-direction shaking table test included a 3500 kg,  $\pm 200$  mm uniaxial hydraulic actuator and a 1500 mm  $\times$  1500 mm square shaking table. The allowable capacity of the specimen was approximately 1000 kg, and the maximum acceleration that could be exerted on the specimen was approximately 1.0 g. Accordingly, a 700-kg load block was constructed by taking into account the weight of the circular and rectangular model specimen of 184 kg and 210 kg, respectively. The vertical axial load was applied by a 3500-kg prestressing force using prestressing strands. The input acceleration for the shaking table test was exerted using the 1940 El Cento earthquake data as shown in Fig. 14. Fig. 23 shows an outline of the shaking table test.

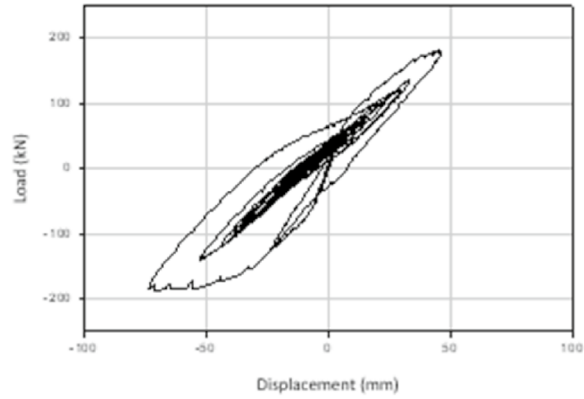
#### 5.1 Test Results and Discussion

##### 5.1.1 Displacement Versus Time Curve

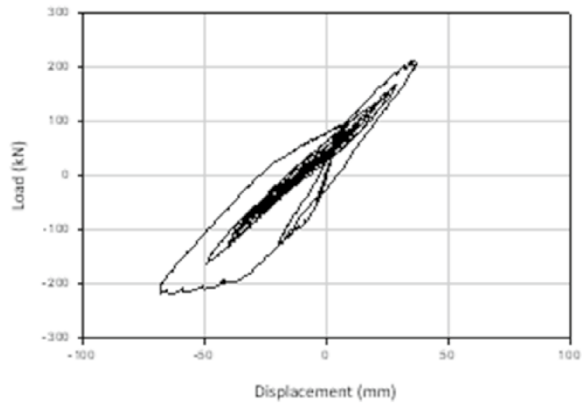
For the shake table test, an acceleration of 0.875 g, 2.5 times the PGA of the El cento earthquake (PGA = 0.35 g), was applied to all specimens. Figs. 24 and 25 show the displacement–time curves obtained from applying 0.875 g on the circular and rectangular specimens during the shaking table test. Table 13 shows the maximum displacement data when the maximum gravity acceleration was applied. Figs. 24 and 25 show the displacement history over time based on the difference in the displacement between the shaking table and the top of the specimen. The calculated relative displacement showed that the maximum displacement for C-RC, C-PU, and C-GFPU specimens were 24.06 mm, 15.82 mm, and 12.40 mm, respectively, suggesting that C-PU and C-GFPU-strengthening reduced the displacement by 34% and 48%, respectively. The calculated relative displacement showed that the maximum displacement for R-RC, R-PU, and R-GFPU specimens were 12.41 mm, 7.63 mm, and 6.71 mm, respectively, suggesting that R-PU and R-GFPU-strengthening reduced the displacement by 35% and 46%, respectively. In overall behavior, PU and GFPU-strengthening reduced the displacement by 34–35% and the 46–48% under El Centro seismic loading, respectively, suggesting that PU is an extremely effective strengthening material.



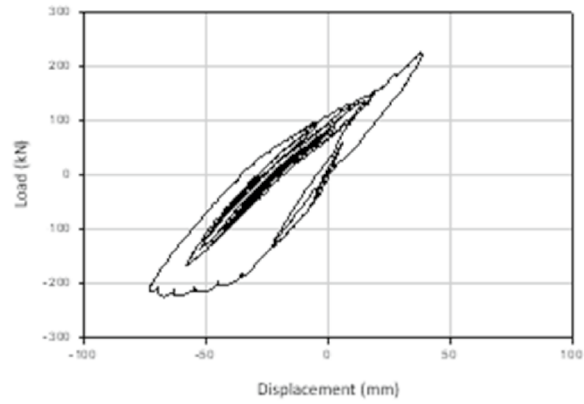
(a) C-RC



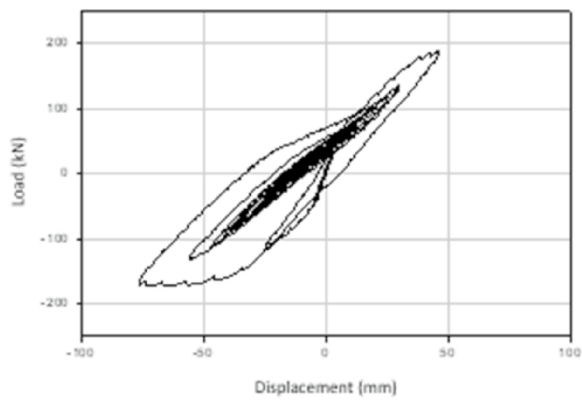
(b) C-PU



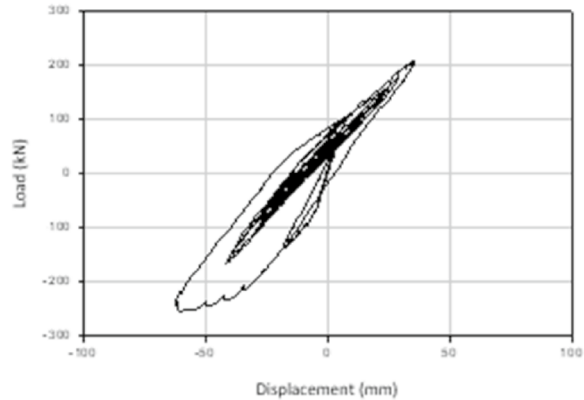
(c) C-GFPU



(d) R-RC

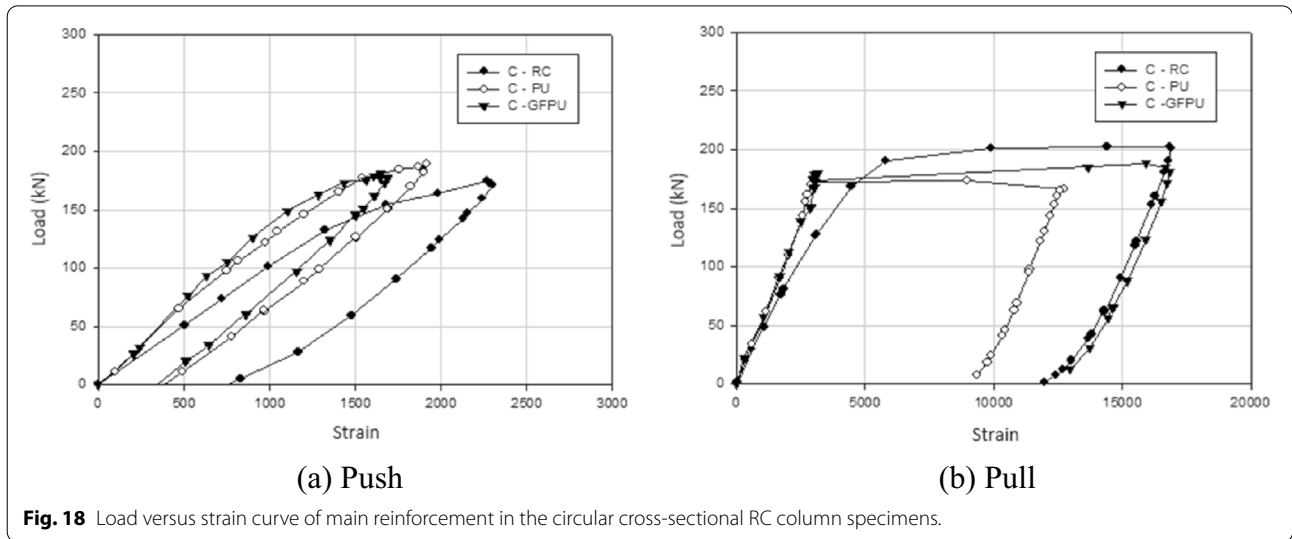
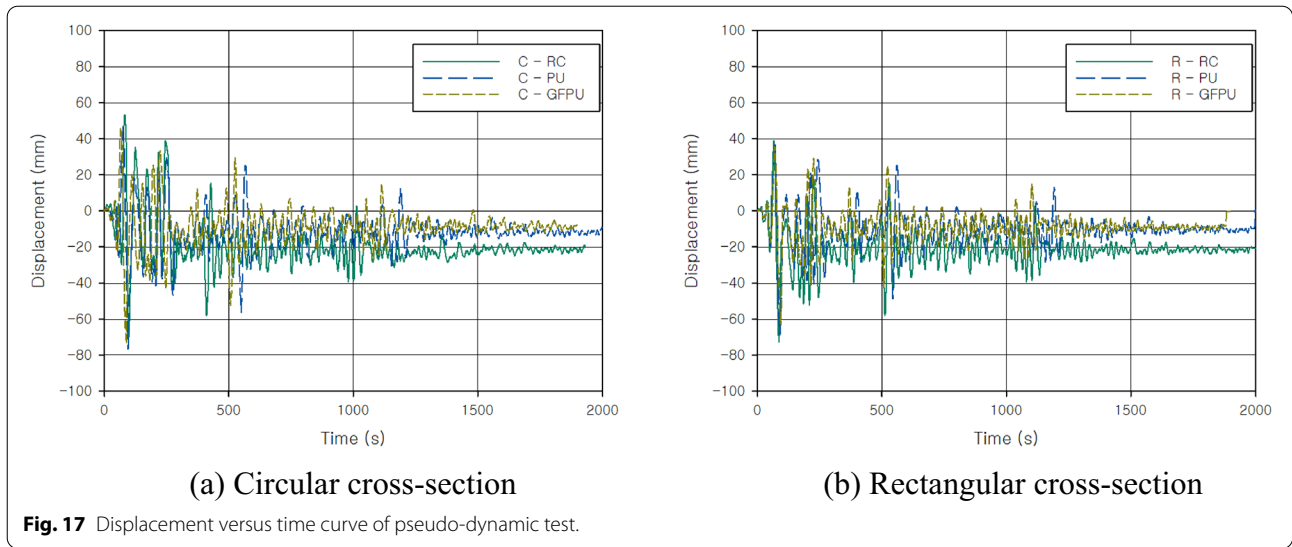


(e) R-PU



(f) R-GFPU

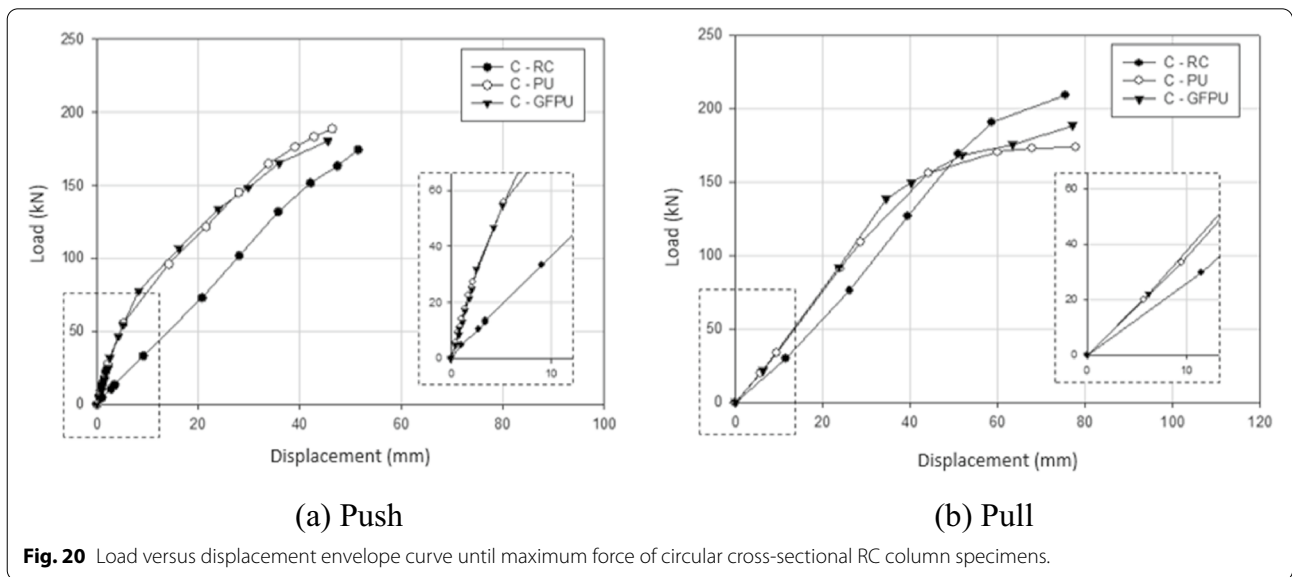
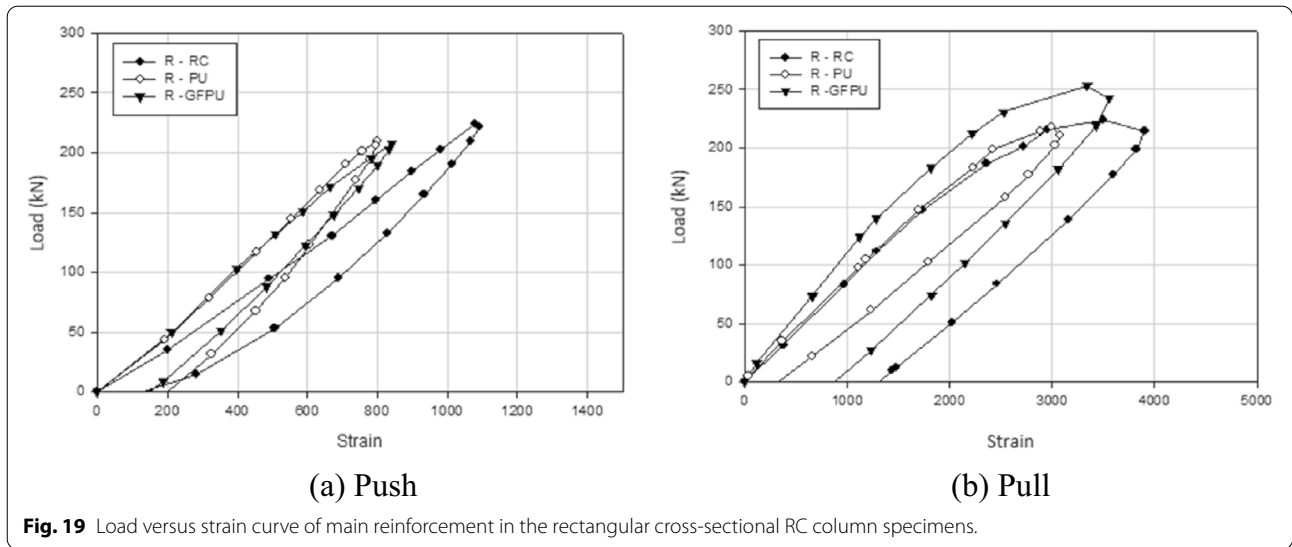
**Fig. 16** Load versus displacement curve of pseudo-dynamic test.



### 5.1.2 Rebar Strain Versus Time Curve

Main reinforcement strain time histories of the circular and rectangular cross-sectional RC column specimens from the shaking table test are shown in Fig. 26. The maximum and minimum strains for all specimens are tabulated in Table 14. The maximum and minimum strains of C-RC, C-PU, and C-GFPU specimens were 0.00242, 0.00123, 0.00163, 0.00054, 0.00062, and 0.00034, respectively. When the strain of main rebar (LS-05) of C-RC reached the yield strain of 0.00242, the strain of main rebars of C-PU and C-GFPU-strengthened specimens were within elastic region. The maximum and minimum strains showed that C-PU and C-GFPU-strengthening reduced the strain by 41% and 74%, respectively,

compared to the non-strengthened specimen. The maximum and minimum strains of R-RC, R-PU, and R-GFPU specimens were 0.00120, 0.00049, 0.00033, 0.00025, 0.00030, and  $-0.00021$ , respectively. When the strain of main rebar (LS-05) of R-RC reached the yield strain of 0.00120, the strain of main rebars of R-PU and R-GFPU-strengthened specimens were within elastic region. The maximum and minimum strains showed that R-PU and R-GFPU-strengthening reduced the strain by 66% and 70%, respectively, compared to the non-strengthened specimens. These results suggest that GFPU-strengthening outperforms PU-strengthening in the circular specimens, whereas PU- and GFPU-strengthening show no significant difference in the rectangular specimens,



although both outperformed the non-retrofitted specimens. The reduction in rebar strain in the RC column specimens with PU- and GFPU-strengthening compared to the non-strengthened specimens suggests that they are effective strengthening materials.

### 6 Conclusions

The seismic performance evaluation of STPU-strengthened RC columns was performed through quasi-static test, pseudo-dynamic test, and shaking table test on scaled model specimens and the experimental results are as follows.

1. From the pseudo-dynamic test, the residual deflection at the load point of the rectangular and circular PU- and GFPU-strengthened specimens decreased by 53.7% and 60.1% and 50.7% and 60.5% compared to non-strengthened specimen, respectively. As expected, the best strengthening performance was observed in the GFPU-strengthened circular column due to the continuous confinement effect from circular cross-sectional shape. Also, the test results showed that the strengthening specimens had higher stiffness than the non-strengthened specimens under seismic loading.

**Table 7** Displacement results according to the maximum load of pseudo-dynamic test.

Specimen	$P_{Max}$ (kN)	Displacement (mm)	Relative displacement (mm)	Ratio
C-RC	-208.63 174.51	-69.48 54.52	124.00	1.00
C-PU	-173.59 188.79	-72.15 46.36	118.51	0.96
C-GFPU	-188.37 180.49	-69.48 45.51	114.99	0.93
R-RC	-224.62 224.07	-67.60 38.29	105.89	1.00
R-PU	-218.09 210.10	-63.53 36.53	100.06	0.94
R-GFPU	-253.13 207.29	-60.56 35.62	96.18	0.91

RC: non-strengthened, C-: circular column, R-: rectangular column.

**Table 8** Strain by specimens according to the maximum load.

Specimen	$P_{Max}$ (kN)	Reinforcement strain ( $\times 10^{-6}$ )	Ratio
C-RC	-208.63 174.51	15,813.94 2266.68	1.00 1.00
C-PU	-173.59 188.79	8986.20 1912.69	0.57 0.84
C-GFPU	-188.37 180.49	15,933.99 1643.11	1.00 0.72
R-RC	-224.62 224.07	3503.03 1079.27	1.00 1.00
R-PU	-218.09 210.10	2998.34 800.11	0.85 0.74
R-GFPU	-253.13 207.29	3344.37 841.81	0.95 0.77

RC: non-strengthened, C-: circular column, R-: rectangular column.

**Table 9** Stress distribution of main reinforcement (circular column).

Applied load (kN)	Push			Pull		
	RC (MPa)	PU (MPa)	GFPU (MPa)	RC (MPa)	PU (MPa)	GFPU (MPa)
0	0.00	0.00	0.00	0.00	0.00	0.00
10	47.38	19.61	23.66	34.63	29.31	28.14
20	64.46	35.61	38.36	90.86	68.89	50.64
30	114.42	-	47.88	121.36	121.67	93.46
40	131.51	63.08	-	170.89	160.38	136.50
50	152.71	82.76	68.86	211.12	194.77	174.14
60	171.09	92.71	-	286.60	224.83	228.86
70	190.56	97.90	89.19	325.54	259.22	252.86
80	213.92	115.21	109.96	364.03	299.45	296.34
90	232.52	133.37	126.18	413.78	332.98	332.24
100	246.36	149.38	140.88	464.39	367.15	369.23
110	274.48	162.79	152.35	513.71	401.76	400.16
120	296.11	191.34	164.68	567.13	426.20	420.27
130	312.11	208.64	188.47	642.83	465.35	459.85
140	332.01	225.51	207.72	702.52	516.61	497.70
150	358.40	257.09	224.80	766.33	527.20	576.00
160	413.77	273.10	247.30	826.46	540.61	595.46
170	464.16	290.83	275.63	892.21	597.71	608.66

*Italic* :exceeded the allowable stress.

**Table 10** Stress distribution of main reinforcement (rectangular column).

Applied load (kN)	Push			Pull		
	RC (MPa)	PU (MPa)	GFPU (MPa)	RC (MPa)	PU (MPa)	GFPU (MPa)
0	0.00	0.00	0.00	0.00	0.00	0.00
10	13.73	14.68	14.15	29.68	14.83	7.25
20	37.52	20.95	–	56.72	40.35	28.01
30	49.42	–	–	74.24	72.15	55.27
40	60.02	38.68	34.91	104.52	97.67	–
50	–	–	42.05	–	108.26	89.66
60	79.27	–	–	137.40	134.00	116.26
70	–	55.77	53.95	167.03	170.99	132.05
80	98.08	63.13	–	194.50	–	–
90	109.33	70.05	69.52	204.44	199.97	165.57
100	117.98	81.73	78.60	221.75	220.95	–
110	131.83	88.86	82.06	257.00	236.74	198.02
120	142.86	91.24	90.93	288.58	270.26	223.75
130	147.61	100.11	99.37	318.43	302.49	241.71
140	155.83	107.46	110.61	338.54	328.66	256.85
150	166.21	112.01	117.10	–	343.15	289.72
160	172.05	118.28	127.27	377.91	367.59	320.00
170	179.19	127.58	132.89	411.21	398.31	344.01
180	188.28	132.99	142.62	441.28	422.96	363.69
190	198.87	142.07	149.54	474.80	463.62	395.49
200	207.09	151.59	160.79	491.02	501.47	424.47
210	217.69	159.37	168.36	579.49	573.50	445.88

Italic: exceeded the allowable stress.

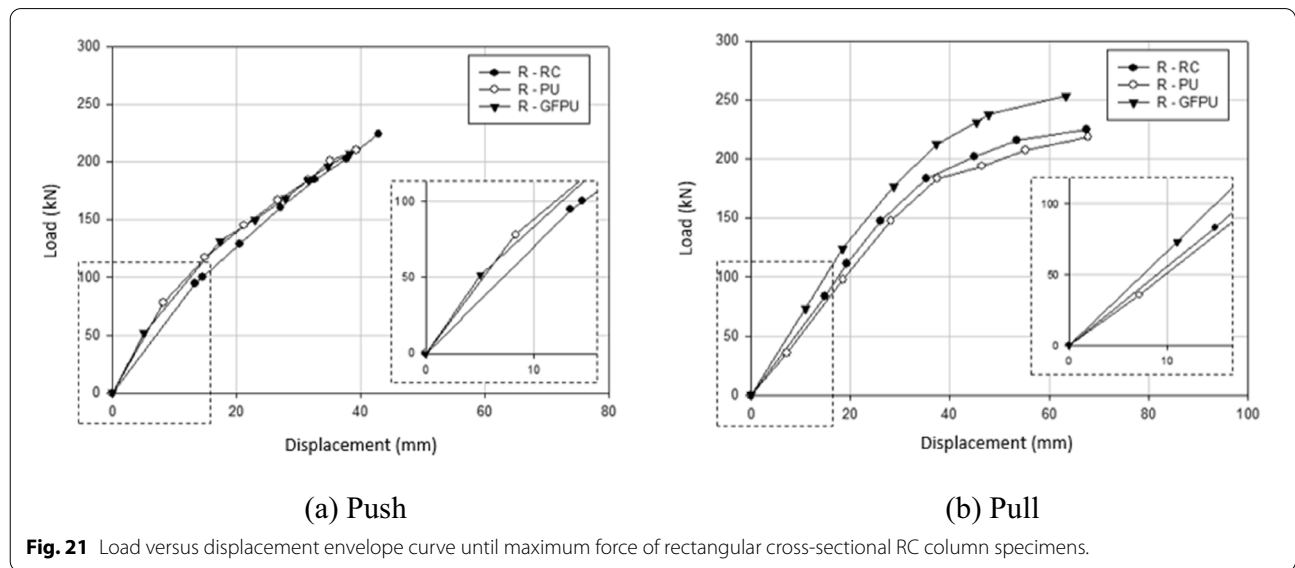




**Fig. 22** Failure behavior of specimens of pseudo-dynamic test.

2. From the pseudo-dynamic test, the displacement ductility of the rectangular and circular PU- and GFPU-strengthened specimens showed 0.93, 0.88 times, 1.16–1.48 and 1.22–1.37 times, respectively, compared to non-strengthened RC specimen. From the pseudo-dynamic test, the energy dissipation of the rectangular and circular specimens with PU- and GFPU-strengthening were 0.83 and 0.74 and 1.53 and 1.52 compared to that of non-strengthened RC specimen, respectively. The reduced ductility of the rectangular specimens comes from the tearing of the strengthening region at the sharp corners in the rectangular cross-section.
3. From the shaking table test, the maximum relative displacement from the rectangular and circular column specimen with PU and GFPU-strengthening was reduced by 35%, 46%, 34%, and 48%, respectively, under El Centro seismic loading, suggesting that PU is an extremely effective strengthening material.
4. From the shaking table test, the maximum and minimum strains of the main rebar from the rectangular and circular specimens with PU- and GFPU-strengthening reduced the strain by 66%, 70%, 41%, and 74%, respectively, compared to the non-strengthened specimens. The reduction in rebar strain in the RC column specimens with PU- and GFPU-strengthening compared to the non-strengthened specimens suggests that they are effective strengthening materials.

**Table 11** Displacement ductility results of pseudo-dynamic test.

Specimen	Load direction	$P_{Max}$ (kN)	Displ. (mm)	Yield displ. (mm)	Displ. ductility	Normalized displ. ductility
C-RC	Push	174.51	54.52	47.26	1.15	1.00
	Pull	-208.63	-69.48	-61.18	1.14	1.00
C-PU	Push	188.79	46.36	34.69	1.34	1.16
	Pull	-173.59	-72.15	-43.03	1.68	1.48
C-GFPU	Push	180.49	45.51	32.39	1.41	1.22
	Pull	-188.37	-69.48	-44.61	1.56	1.37
R-RC	Push	224.07	38.29	31.93	1.20	1.00
	Pull	-224.62	-67.60	-40.18	1.68	1.00
R-PU	Push	210.10	36.53	27.58	1.32	1.10
	Pull	-218.09	-63.53	-40.64	1.56	0.93
R-GFPU	Push	207.29	35.62	28.54	1.25	1.04
	Pull	-253.13	-60.56	-40.74	1.49	0.88

\* RC: non-strengthened, C-: circular column, R-: rectangular column.

**Table 12** Dissipation energy results of pseudo-dynamic test.

Specimen	Dissipation energy (kN mm)	Ratio
C-RC	6828.68	1.00
C-PU	10,425.61	1.53
C-GFPU	10,379.11	1.52
R-RC	12,292.94	1.00
R-PU	10,201.87	0.83
R-GFPU	9153.05	0.74

\* RC: non-strengthened, C-: circular column, R-: rectangular column.

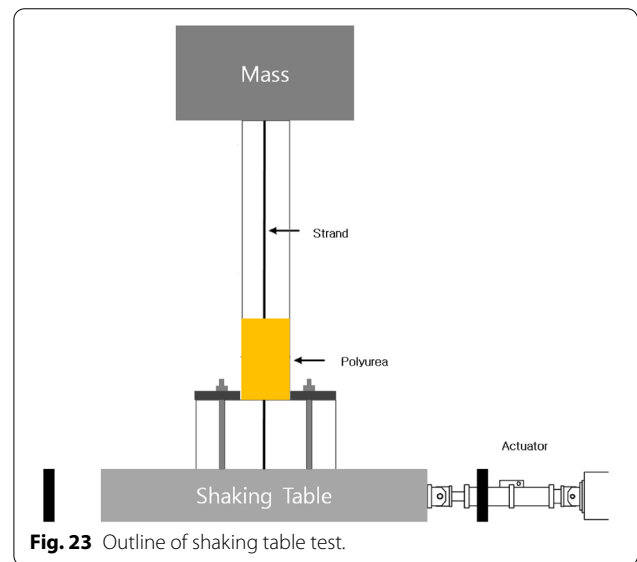
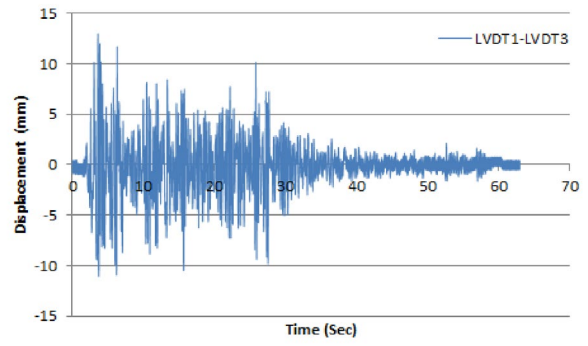
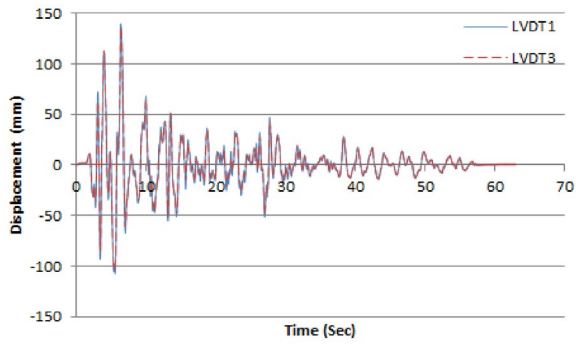


**Fig. 23** Outline of shaking table test.

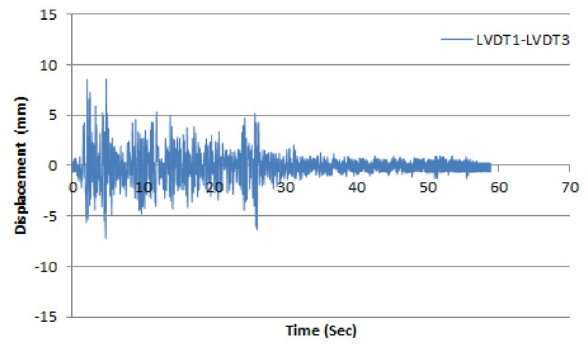
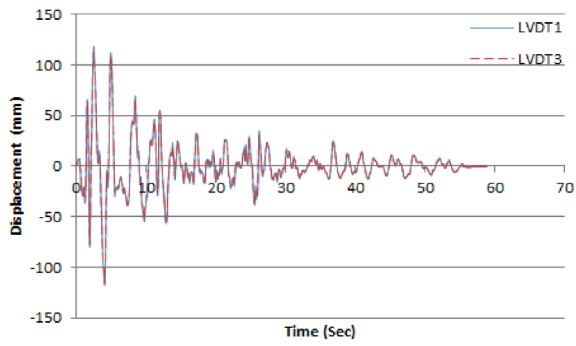
**Table 13** Maximum displacement and relative displacement results of shaking table test.

Specimen	Shaking table (mm)	Column head (mm)	Relative displ. (mm)	Range of relative displ. (mm)	Ratio
C-RC	136.55	139.97	12.96	24.06	1.00
	-103.39	-107.46	-11.10		
C-PU	112.84	118.37	8.59	15.82	0.66
	-116.26	-117.86	-7.23		
C-GFPU	127.56	133.14	7.43	12.40	0.52
	-107.72	-107.36	-4.97		
R-RC	134.00	140.17	7.49	12.41	1.00
	-105.40	-105.96	-4.92		
R-PU	134.59	138.86	5.57	7.63	0.65
	-105.10	-104.55	-2.06		
R-GFPU	134.49	137.41	4.92	6.71	0.54
	-104.75	-104.70	-1.79		

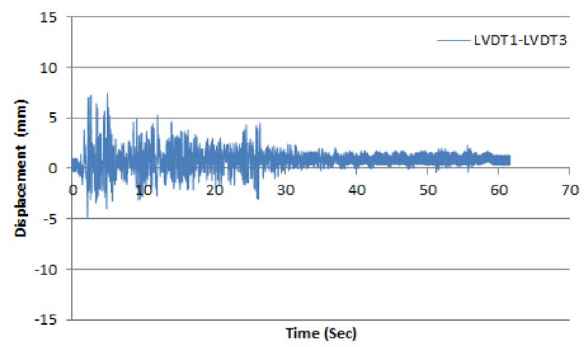
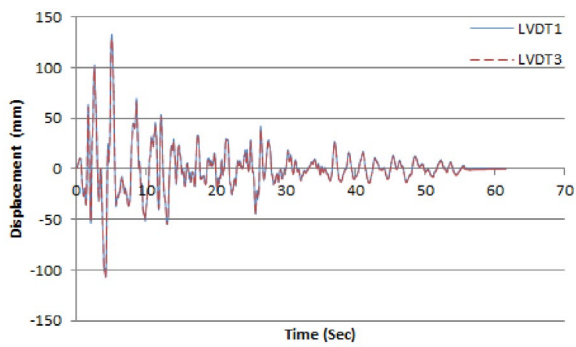
RC: non-strengthened, C-: circular column, R-: rectangular column.



(a) C-RC

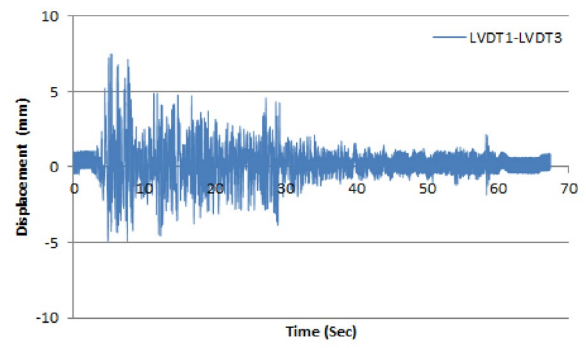
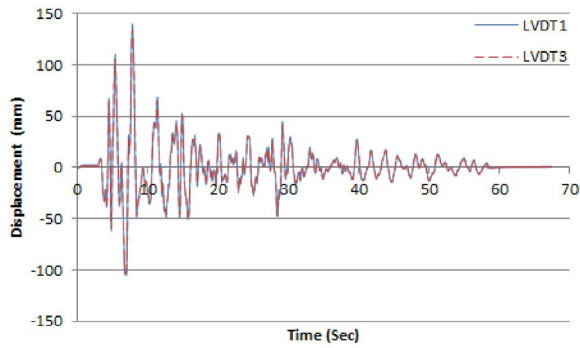


(b) C-PU

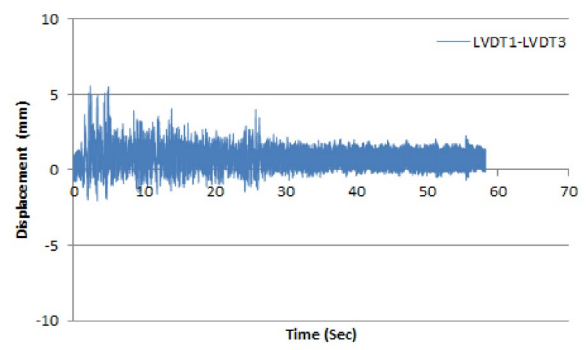
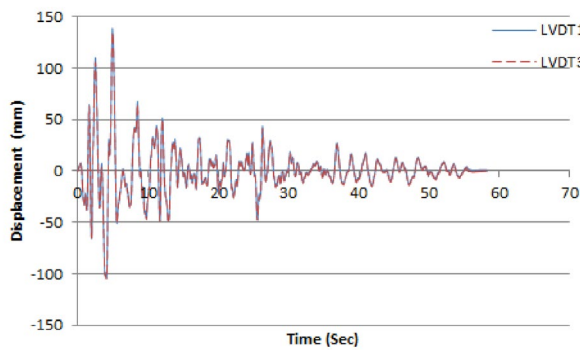


(c) C-GFPU

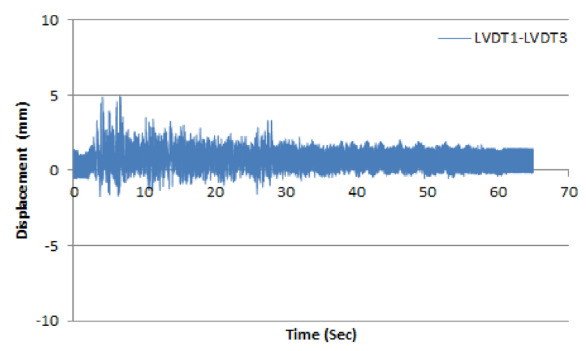
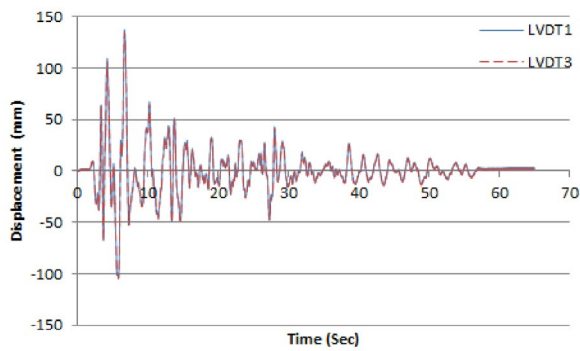
**Fig. 24** Displacement time history of the circular cross-sectional RC column specimens.



(a) R-RC

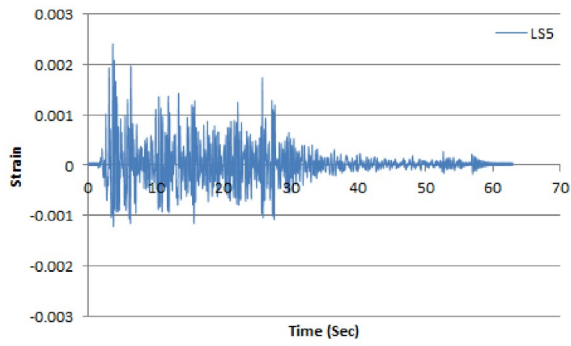


(b) R-PU

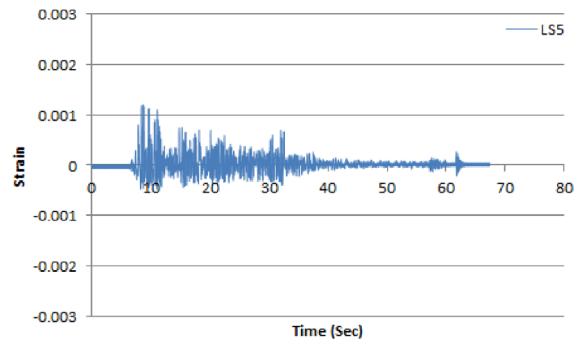


(c) R-GFPU

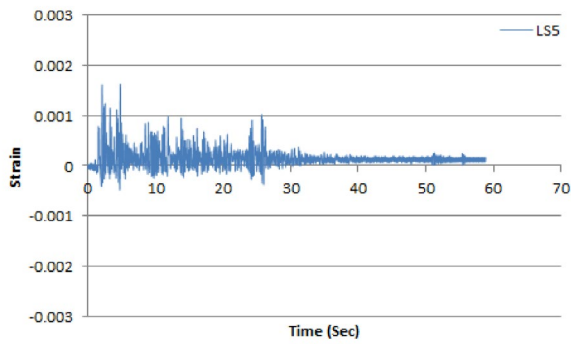
**Fig. 25** Displacement time history of the rectangular cross-sectional RC column specimens.



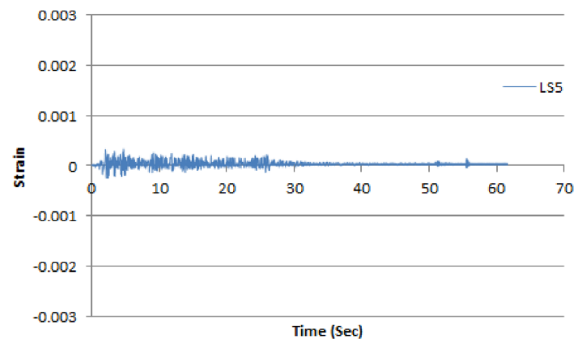
(a) C-RC



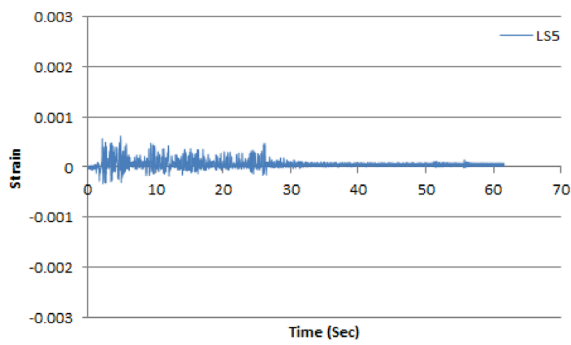
(b) R-RC



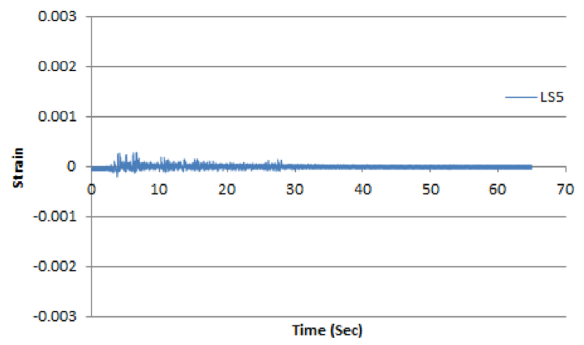
(c) C-PU



(d) R-PU



(e) C-GFPU



(f) R-GFPU

**Fig. 26** Main reinforcement strain time history of the circular and rectangular cross-sectional RC column specimens.

**Table 14** Maximum and minimum reinforcement strain results of shaking table test.

Specimen	Reinforcement strain ( $\times 10^{-6}$ )	Range of strain ( $\times 10^{-6}$ )	Ratio
C-RC	2420 – 1230	3650	1.00
C-PU	1630 – 540	2170	0.59
C-GFPU	620 – 340	960	0.26
R-RC	1200 – 490	1690	1.00
R-PU	330 – 250	580	0.34
R-GFPU	300 – 210	510	0.30

RC: non-strengthened, C-: circular column, R-: rectangular column.

#### Acknowledgements

This work is supported by the Korea Agency for Infrastructure Technology Advancement (KAIA) grant funded by the Ministry of Land, Infrastructure and Transport (Grant 21CFRP-C163382-01).

#### Author contributions

T-HL performed most of test and analysis works; main writer of the paper. S-JC supported the research project and writing the paper. D-HY advised the research test method of the paper. J-HJK is the PI of the research project, who planned and developed the main idea of the study. All authors read and approved the final manuscript.

#### Authors' information

Tae-Hee Lee, Doctoral Student, School of Civil and Environmental Engineering, Yonsei University, Republic of Korea.  
Seung-Jai Choi, Postdoctoral Student, Ph.D., School of Civil and Environmental Engineering, Yonsei University, Republic of Korea.  
Dal-Hun Yang, Postdoctoral Student, Ph.D., Department of Structural Engineering Research, Korea Institute of Civil Engineering and Building Technology, Republic of Korea.  
Jang-Ho Jay Kim, Professor, Ph.D., School of Civil and Environmental Engineering, Yonsei University, Republic of Korea.

#### Funding

Ministry of Land, Infrastructure and Transport (Grant 21CFRP-C163382-01).

#### Availability of data and materials

Not applicable.

#### Declarations

#### Ethics approval and consent to participate

Not applicable.

#### Consent for publication

Not applicable.

#### Competing interests

The authors declare that they have no competing interests.

#### Author details

<sup>1</sup>School of Civil and Environmental Engineering, Yonsei University, 50, Yonsei-ro, Seodaemun-gu, Seoul 03722, Republic of Korea. <sup>2</sup>Central

Research Institute, Korea Hydro & Nuclear Power Co., Ltd., 70, Yuseong-daero 1312beon-gil, Yuseong-gu, Daejeon, Republic of Korea.

Received: 21 February 2022 Accepted: 25 July 2022

Published online: 01 December 2022

#### References

- Almusallam, T., Al-Salloum, Y., Elsanadedy, H., Alshenawy, A., & Iqbal, R. (2018). Behavior of FRP-strengthened RC beams with large rectangular web openings in flexure zones: Experimental and numerical study. *International Journal of Concrete Structures and Materials*, 12(5), 739–766.
- Ang, B. G., Priestley, M. J. N., & Paulay, T. (1989). Seismic shear strength of circular reinforced concrete columns. *ACI Structural Journal*, 86(1), 45–59.
- Bonacci, J. F., & Maalej, M. (2001). Behavioral trends of RC beams strengthened with externally bonded FRP. *Journal of Composites for Construction*, 5(2), 102–113.
- Chen, C. H., Lai, W. C., Cordova, P., Deierlein, G. G. & Tsai, K. C. (2003). Pseudo-dynamic test of full-scale RCS frame: Part 1-Design, construction and testing. In *Proceedings of International Workshop on Steel and Concrete Composite Constructions* (pp. 107–118).
- Chen, Z. F., Wan, L. L., Lee, S., Ng, M., Tang, J. M., Liu, M., & Lee, L. (2008). Evaluation of CFRP, GFRP and BFRP material systems for the strengthening of RC slabs. *Journal of Reinforced Plastics and Composites*, 27(12), 1233–1243.
- Chung, L., Hur, M. W., & Park, T. W. (2018). Performance evaluation of CFRP reinforced concrete members utilizing fuzzy technique. *International Journal of Concrete Structures and Materials*, 13(2), 183–193.
- Chung, Y. S., Park, J. H., Park, H. S., & Cho, C. B. (2002). Pseudo dynamic test for the seismic performance enhancement of circular RC Bridge Piers retrofitted with fibers. *Journal of the Korea Concrete Institute*, 14(2), 180–189. In Korea.
- Huang, W. B., Xiang, J. Y., Lv, P., & Li, X. M. (2012). Study on mechanical properties aging of spray pure polyurea for hydraulic concrete protection. *Advanced Materials Research*, 374, 1325–1329.
- Jin, D. H. (2016). Seismic performance evaluation of concrete structure using hybrid test system, Master degree thesis, Myungji University. (In Korea).
- Jung, R. Y., & Benson, S. P. (2006). Performance evaluation of a real-time pseudo-dynamic test system. *Earthquake Engineering and Structural Dynamics*, 35(7), 789–810.
- Kim, D. K., Kim, D. Y., Ahn, J. H., & Park, C. L. (1997). Assessment of the seismic capacity of structure using pseudo dynamic test. *Journal of the Earthquake Engineering Society of Korea*, 1(2), 49–57. In Korea.
- Kim, J. S., Kwon, M. H., Seo, H. S., Lim, J. H., & Kim, D. Y. (2013). An experimental study on seismic performance evaluation of retrofitted column of FRP seismic reinforcement that can be emergency construction. *Journal of the Korea Institute for Structural Maintenance and Inspection*, 17(6), 21–30. In Korea.
- KMA, Korea Meteorological Administration, Earthquake. (2016). Retrieved from <http://www.kma.go.kr/mini/earthquake/main.jsp>. (In Korea).
- Lee, D. H., Oh, J. K., Yu, W. D., & Choi, E. S. (2012). Seismic performance of RC columns confined by outside lateral reinforcement. *Journal of the Korean Society of Civil Engineers*, 32(3), 189–196. In Korea.
- Chen, Z. F., Wan, L. L., Lee, S., Ng, M., Tang, J. M., Liu, M., & Lee, L. (2008). Evaluation of CFRP, GFRP and BFRP material systems for the strengthening of RC slabs. *Journal of Reinforced Plastics and Composites*, 27, 1233–1243.
- Li, Y. F., Chang, S. Y., Tzeng, W. C., & Huang, K. (2003). The pseudo dynamic test of RC bridge columns analyzed through the Hilbert–Huang transform. *Journal of Mechanics*, 19(3), 373–387.
- Lu, X. Z., Teng, J. G., Ye, L. P., & Jiang, J. J. (2005). Bond-slip models for FRP sheets/plates bonded to concrete. *Engineering Structures*, 27(6), 920–937.
- MacRae, G. A., & Kawashima, K. (1997). Post-earthquake residual displacements of bilinear oscillators. *Earthquake Engineering & Structural Dynamics*, 26(7), 701–716.
- Marriott, D., Pampanin, S., & Palermo, A. (2009). Quasi-static and pseudo-dynamic testing of unbonded post-tensioned rocking bridge piers with external replaceable dissipaters. *Earthquake Engineering and Structural Dynamics*, 38(3), 331–354.

- Shing, P. S. B., & Vannan, M. T. (1991). Implicit time integration for pseudo dynamic tests: convergence and energy dissipation. *Earthquake Engineering and Structural Dynamics*, 20(9), 809–819.
- Truong, G. T., Dinh, N. H., & Kim, J. C. (2017). Seismic performance of exterior RC Beam–column joints retrofitted using various retrofit solutions. *International Journal of Concrete Structures and Materials*, 11(3), 415–433.
- Yang, Y. S., Wang, K. J., Wang, S. J., Hsu, C. W., Tsai, K. C. & Hsieh, S. H. (2004). Networked pseudo-dynamic testing part I: Database approach, In *Proceedings of the 13th World Conference on Earthquake Engineering*, Vancouver, BC, Canada (pp. 1910–1919).
- Youm, K. S., Kwon, T. G., Lee, Y. H., & Hwang, Y. K. (2006). Seismic retrofit of GFRP wrapping on the lap-spliced bridge piers. *Journal of the Korean Society of Civil Engineers*, 26(2), 311–318. In Korea.
- Zhang, Q., Zhang, P. P., & Jiao, Q. Z. (2006). Synthesis and characterization of microcapsules with chlorpyrifos cores and polyurea walls. *Chemical Research in Chinese Universities*, 22(3), 379–382.

### Publisher's Note

Springer Nature remains neutral with regard to jurisdictional claims in published maps and institutional affiliations.

Submit your manuscript to a SpringerOpen<sup>®</sup> journal and benefit from:

- ▶ Convenient online submission
- ▶ Rigorous peer review
- ▶ Open access: articles freely available online
- ▶ High visibility within the field
- ▶ Retaining the copyright to your article

---

Submit your next manuscript at ▶ [springeropen.com](https://www.springeropen.com)

---